CONTROLLED DOXORUBICIN DELIVERY FROM PHOTORESPONSIVE LIPOSOMES CARRYING VITAMIN A DERIVATIVES

A THESIS SUBMITTED TO
THE GRADUATE SCHOOL OF NATURAL AND APPLIED SCIENCES
OF
MIDDLE EAST TECHNICAL UNIVERSITY

BY

SENEM HEPER

IN PARTIAL FULFILLMENT OF THE REQUIREMENTS
FOR
THE DEGREE OF MASTER OF SCIENCE
IN
BIOTECHNOLOGY

SEPTEMBER 2014

Approval of the thesis:

CONTROLLED DOXORUBICIN DELIVERY FROM PHOTORESPONSIVE LIPOSOMES CARRYING VITAMIN A DERIVATIVES

submitted by **SENEM HEPER** in partial fulfillment of the requirements for the degree of **Master of Science in Department of Biotechnology, Middle East Technical University** by,

Prof. Dr. Canan Özgen _____
Dean, Graduate School of **Natural and Applied Sciences**

Prof. Dr. Filiz Bengü Dilek _____
Head of Department, **Biotechnology**

Prof. Dr. Vasıf Hasırcı _____
Supervisor, **Biology Dept., METU**

Prof. Dr. Nesrin Hasırcı _____
Co-Supervisor, **Chemistry Dept., METU**

Examining Committee Members:

Prof. Dr. Tülin GÜRAY _____
Biology Dept., METU

Prof. Dr. Vasıf Hasırcı _____
Biology Dept., METU

Prof. Dr. Menemşe Gümüşderelioğlu _____
Chemical Engineering Dept., Hacettepe University

Assoc. Prof. Dr. Mayda Gürsel _____
Biology Dept., METU

Assoc. Prof. Dr. Çağdaş D. Son _____
Biology Dept., METU

Date: 04.09.2014

I hereby declare that all information in this document has been obtained and presented in accordance with academic rules and ethical conduct. I also declare that, as required by these rules and conduct, I have fully cited and referenced all material and results that are not original to this work.

Name, Last Name: Senem Heper

Signature:

ABSTRACT

CONTROLLED DOXORUBICIN DELIVERY FROM PHOTORESPONSIVE LIPOSOMES CARRYING VITAMIN A DERIVATIVES

Heper, Senem
M.S., Department of Biotechnology
Supervisor: Prof. Dr. Vasıf Hasırcı
Co-Supervisor: Prof. Dr. Nesrin Hasırcı
September 2014, 73 pages

Drug delivery systems (DDS) have been an attractive approach to eliminate the drawbacks of conventional drug administration. Controlled and photoresponsive drug delivery systems have a special advantage; they deliver drugs more effectively. Liposomes are mostly preferred as drug carriers due to their ability to carry both hydrophilic and hydrophobic drugs, their being non-toxic and non-immunogenic.

In this study, photoresponsive liposomes were prepared by incorporating vitamin A derivatives into the lipid bilayer of the liposomes for use in treatment of eye diseases that require frequent and continuous drug administration. Proliferative vitreoretinopathy was selected as a model disease and doxorubicin as the therapeutic agent. Doxorubicin loaded phosphatidyl choline (PC): cholesterol (CHOL): all-trans retinal (ATR) (7:1:3) liposomes were tested on RPE/D407 cells to determine the effect of UVA exposure (365 nm) on the release of doxorubicin, and therefore, cell viability. Among the different liposome compositions studied by exposing to UVA it was found that PC:CHOL:ATR (7:1:3) formulation responded the best. Antiproliferative effects of all-trans retinal (ATR) and doxorubicin were observed

when tested on RPE/D407 cell line. Also, the interaction of the cells with doxorubicin and liposomes were studied with flow cytometry and confocal laser scanning microscopy (CLSM). It was found that liposomes or ATR can penetrate the cells while doxorubicin penetrates the nucleus.

Keywords: Photoresponsive liposomes, Controlled drug delivery, All-trans retinal, Proliferative vitreoretinopathy, Doxorubicin

ÖZ

VİTAMİN A TÜREVİ İÇEREN IŞIĞA DUYARLI LİPOZOMLARDAN KONTROLLÜ DOXORUBICIN SALIMI

Heper, Senem
Yüksek Lisans, Biyoteknoloji Bölümü
Tez Yöneticisi: Prof. Dr. Vasıf Hasırcı
Ortak Tez Yöneticisi : Prof. Dr. Nesrin Hasırcı
Eylül 2014, 73 sayfa

İlaç salım sistemleri, geleneksel ilaç uygulamasında karşılaşılan problemlerin üstesinden gelinmesine yönelik çekici bir yaklaşımdır. Kontrollü ve ışığa duyarlı ilaç salım sistemleri özel bir avantaja sahiptir: ilaçları daha etkin salarlar. Lipozomlar sıklıkla tercih edilen ilaç taşıyıcılardır, çünkü hem hidrofilik hem de hidrofobik ilaçları taşıyabilirler, toksik ve immünojenik değildirler.

Bu çalışmada, sık ve devamlı ilaç uygulaması gerektiren göz hastalıklarının tedavisi için lipozomların çift katmanlı lipid yapısına vitamin A türevleri eklenerek ışığa duyarlı lipozomlar hazırlanmıştır. Proliferatif vitreoretinopati (PVR) model bir hastalık ve doxorubicin ise terapötik ajan olarak seçilmiştir. Doxorubicin yüklü PC:CHOL:ATR (7:1:3) lipozomlar, UVA'ya (365 nm) maruz bırakılmanın doxorubicin salımı ve dolayısıyla hücre canlılığı üzerine etkisini belirlemek için RPE/D407 hücreleri üzerinde denenmiştir. UVA'ya maruz bırakılarak incelenen farklı lipozom kompozisyonları arasında PC:CHOL:ATR (7:1:3) formülasyonun en iyi tepki veren olduğu bulunmuştur. All-trans retinal (ATR) ve doxorubicin RPE/D407 hücreleri üzerinde denendiğinde antiproliferatif etkileri olduğu gözlenmiştir. Ayrıca, doxorubicin ve lipozomların hücreler ile olan etkileşimleri akış

sitometrisi ve konfokal lazer taramalı mikroskopi ile incelenmiştir. Doxorubicin'in hücrelerin çekirdeğine girdiği ve lipozomların ya da ATR'in ise hücrenin içine girdiği bulunmuştur.

Anahtar Kelimeler: Işığa duyarlı lipozomlar, Kontrollü ilaç salımı, All-trans retinal, Proliferatif Vitreoretinopati, Doxorubicin

Dedicated to my family

ACKNOWLEDGEMENTS

I would like to express my deepest gratitude to my supervisor Prof. Dr. Vasıf Hasırcı for his continuous guidance, advice, support, encouragement and insight throughout my thesis.

I am also grateful to my co-supervisor Prof. Dr. Nesrin Hasırcı for her support, guidance, useful comments and suggestions.

I would like to express my special thanks to Dr. Arda Büyüksungur for his patience, endless support and help and being there for me all the time I needed him throughout this thesis.

I would also like to thank my friends Deniz Sezlev Bilecen, Damla Arslantunalı, Aysu Küçükturhan, Gözde Eke, Menekşe Ermiş Şen and Fatih Şen for being like a family on my worst day.

I would like to thank all the members of BIOMATEN-METU Center of Excellence in Biomaterials and Tissue Engineering and my labmates, Aylin Kömez, Büşra Günay, Ezgi Antmen, Bilgenur Kandemir, Ayla Şahin, Onur Hastürk, Esen Sayın, Tuğba Dursun, Sepren Öncü, Cemile Kılıç, Ayşe Selcen Alagöz, Gökhan Bahçecioğlu, Assoc. Prof. Dr. Erkan Türker Baran and our technician Zeynel Akın for their support in this study.

I would like to express my special thanks to my friend Özlem Sarı for her friendship, endless help, support and understanding throughout my study.

I owe special thanks to my best friends, my beloved sisters Bengü Aktaş and Sıla Yardım for their invaluable friendship, continuous help and support.

Finally, I would like to express my deepest gratitude to my precious family Seval Heper, Ali Heper, Ogün Heper and Seven Heper for their understanding, limitless love, caring, support, patience and trust in me not only for this study, but for all my life.

TABLE OF CONTENTS

LIST OF TABLES

TABLES

LIST OF FIGURES

FIGURES

LIST OF ABBREVIATIONS

9-CR	9-cis Retinal
ATR	All-trans Retinal
BRB	Blood-Retinal Barrier
CALCEIN	(3, 3'-Bis [N, N-bis (carboxymethyl) aminomethyl] fluorescein)
CLSM	Confocal Laser Scanning Microscope
DDS	Drug Delivery System
DMEM	Dulbecco's Modified Eagle Medium
DMSO	Dimethyl Sulfoxide
DNA	Deoxyribonucleic Acid
DOPC	1,2-dioleoyl-sn-glycero-3-phosphocholine
DRV	Dehydration-Rehydration Vesicles
DSPC	1,2-distearoyl-sn-glycero-3-phosphocholine
EDTA	Ethylene Diamine Tetraacetic Acid
EE	Encapsulation Efficiency
FBS	Fetal Bovine Serum
LUV	Large Unilamellar Vesicles
MLV	Multilamellar Vesicles
MVV	Multivesicular Vesicles
MWCO	Molecular Weight Cut-off
PBS	Phosphate Buffer Saline
PE	Phosphatidylethanolamine
PEG	Polyethylene Glycol
PC	Phosphatidylcholine
PS	Phosphatidylserine
PVR	Proliferative Vitreoretinopathy
RA	Retinoic Acid
RD	Retinal Detacment
RPE	Retinal Pigment Epithelial

SUV	Small Unilamellar Vesicles
TLF	Thin Lipid Film
UV	Ultraviolet

CHAPTER 1

INTRODUCTION

1.1 Proliferative Vitreoretinopathy (PVR)

Vision is the sense which provides the organism information about the state of the world and the major organ of vision is the eye. Light rays reflect from objects and enter the eyes through the cornea and then are focused on the retina which contains millions of nerve cells called cones and rods. These cells convert the light into electrical impulses which are sent to the brain via optic nerves. Finally, visual perception occurs in the brain. The anatomy of the eye and the retina is shown in Figure 1.

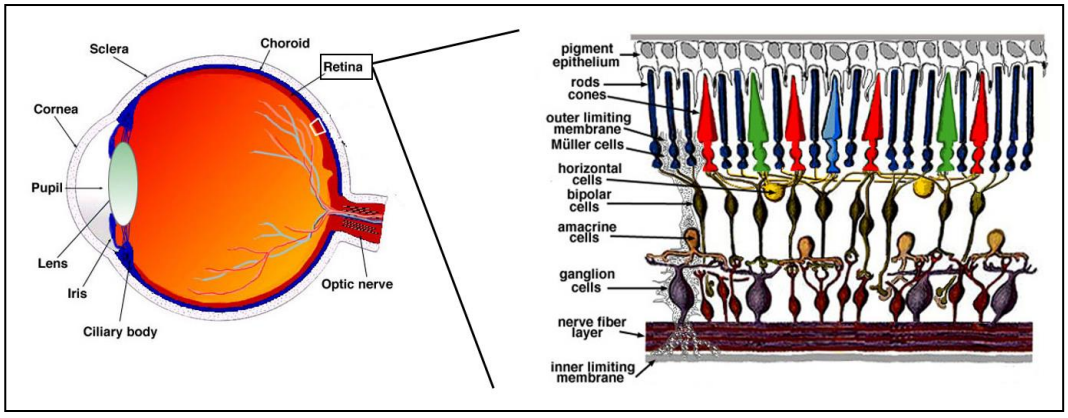

Figure 1. Anatomy of the eye and the retina (Adapted from http://webvision.med.utah.edu/book/part-i-foundations/simple-anatomy-of-the-retina/).

Retina Society Terminology Committee coined the term "proliferative vitreoretinopathy" PVR in 1983 (Tosi et. al., 2014). According to this classification the term "proliferative" refers to its pathogenesis, while the term "vitreoretinopathy" implies the location of the disease (Pastor, 1998). It was thought that PVR is more than a specific clinical picture, it can occur as a result of many different intraocular disorders (e.g. trauma, multiple or giant lacerations, uveitis, retinal detachments and surgery of retinal detachments) (Bozan et. al., 2004).

Failure in retinal reattachment surgery is one of the major causes of PVR (75%) (Sadaka et. al., 2012). In fact, PVR is an abnormal wound healing process and is characterized by cell proliferation, membrane formation and traction on both surfaces of retina (Charteris, 1995). Contraction of these membranes causes retinal detachment (RD). PVR is one of the most important problem in ophthalmology because it may result in irreversible vision loss (Tosi et. al., 2014).

1.1.1 Classification of Proliferative Vitreoretinopathy

Classification of PVR is important for defining the signs in patients before the surgery and post-operative period. Also, it helps to determine the effect of therapies performed during clinical trials. Although the classification which was published by Retina Society Terminology Committee in 1983 is still valid today, it has some limitations. For instance, it does not refer to the degree of cellular proliferative activity and also to the location of the PVR. Therefore, the 1983 classification was revised in a way to include locations and types of contractions (Pastor, 1998), so that we can now understand the localization of the pathobiology of PVR. These classifications are summarized in Table 1.

Table 1. Classification of PVR (Adapted from Pastor et. al., 1998).

A. Retina Society Classification (1983)

Grade	Name	Clinical Characteristics
A	Minimal	Vitreous haze, vitreous pigment clumps
B	Moderate	Wrinkling of the inner retinal surface, rolled edge of retinal break, retinal stiffness, vessel tortuosity
C	Marked	Full thickness fixed retinal folds
C1		One quadrant
C2		Two quadrants
C3		Three quadrants
D	Massive	Fixed retinal folds in four quadrants
D1		Wide funnel shape
D2		Narrow funnel shape
D3		Closed funnel

B. Updated Proliferative Vitreoretinopathy Grade Classification (1991)

Grade	Clinical Characteristics
A	Vitreous haze, vitreous pigment clumps
B	Wrinkling of the inner retinal surface, retinal stiffness, rolled and irregular edge of retinal break, decreased mobility of vitreous
CP 1–12	Diffuse or starfolds in posterior to equator and/or subretinal strands
CA 1–12	Focal, diffuse, perpendicular or circumferential folds, anterior displacement, condensed vitreous strands in anterior to equator

C. Updated Proliferative Vitreoretinopathy Contraction Type Classification (1991)

Type	Location (in relation to equator)	Features
Focal	Posterior	Starfold
Diffuse	Posterior	Confluent star folds posterior to vitreous base; optic disc may not be visible
Subretinal	Posterior/anterior	Proliferation under the retina; annular strand near disc
Circumferential	Anterior	Contraction along posterior edge of vitreous base with central displacement of the retina, peripheral retina stretched
Anterior	Anterior	Vitreous base pulled anteriorly by proliferative tissue, displacement ciliary processes may be stretched, iris retracted

Different classifications of PVR (with the photographs of patients) according to the updated grade classification (1991) are shown in Figure 2.

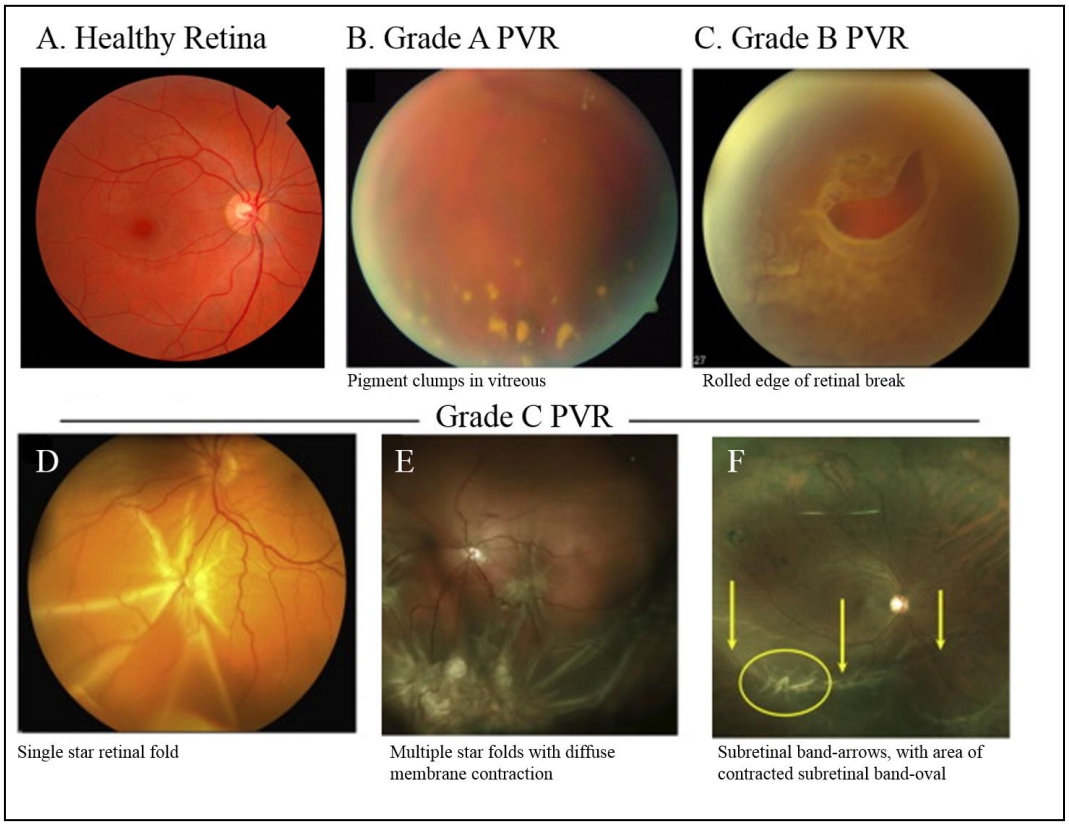

Figure 2. Photographs of grades of PVR (Adapted from Pennock et al, 2014).

1.1.2 Cell Types Involved: Pathobiology

It is critically important to understand the pathophysiological mechanism of PVR in order to design the type of therapy. Although the whole process of PVR has not been fully understood yet, it is well known that PVR is a wound healing process with an abnormal path (Garweg et. al., 2013). Therefore, progression of PVR can be summerized into three phases like a normal wound healing: Inflammation, proliferation and modulation of scar (contraction). There are four major cell types involved in PVR: Retinal pigment epithelial (RPE) cells, glial cells, fibroblastic cells and inflammatory cells (macrophages and lymphocytes). These cells migrate to the vitreous cavity of the eye and lead to membrane formation in periretinal area and eventually contraction and traction of these newly formed membranes cause retinal detacment (Umazume et al., 2013). Figure 3 presents the schematic illustration of PVR process.

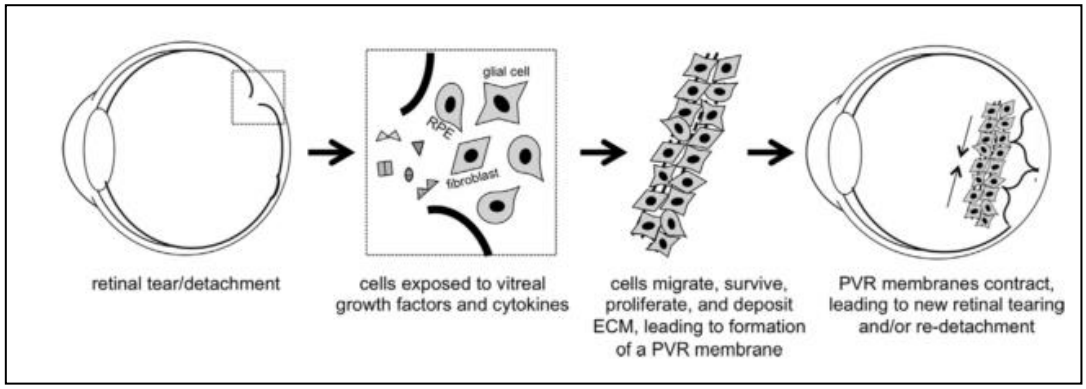

Figure 3. Schematic illustration PVR process (Pennock et al., 2014).

Blood-retinal barrier (BRB) generally breaks down after trauma. This is the first and the most important initiator of the development of PVR which induces cell migration and proliferation (Tosi et al., 2014). Pathobiology of PVR is shown in Figure 4. Studies with light microscopy, electron microscopy and immunohistochemistry, indicated that RPE cells show a higher proliferation feature in comparision to other cell types in PVR. It is also known that RPE cells differentiate into macrophages or fibroblast-like morphology (Charteris, 1995). Also, glial cells proliferate and contribute to periretinal membrane formation. It was shown that simple glial epiretinal membranes cause retinal breaks. However, according to immunohistochemical studies, purely glial membranes are non-tractional, therefore it is necessary that other cellular components to be contractile and tractional features of periretinal membranes in PVR. Additionally, studies in the literature indicate that some growth factors and cytokines have a significant influence on migration, proliferation and differentiation of the cells. These growth factors include platelet-derived growth factor (PDGF), transforming growth factor beta (TGF-β), epidermal growth factor (EGF) and fibroblast growth factor (FGF). Also, interleukins (IL-1, IL-6, IL-8, IL-10) and interferon-gamma (INF-γ) are important cytokines in PVR (Morescalchi et al., 2013).

In the literature, there are *in vitro* and *in vivo* studies carried out with rabbits shows that proliferation and migration of RPE and glial cells on both sides of the detached retina, contributes the poor recovery of vision. Also, the separation of the outer retina induces ischemia (locational anemia and oxygen deficiency) which causes death of

photoreceptors by necrosis or apaptosis, therefore, contributes the vision loss, too (Garweg et al., 2013).

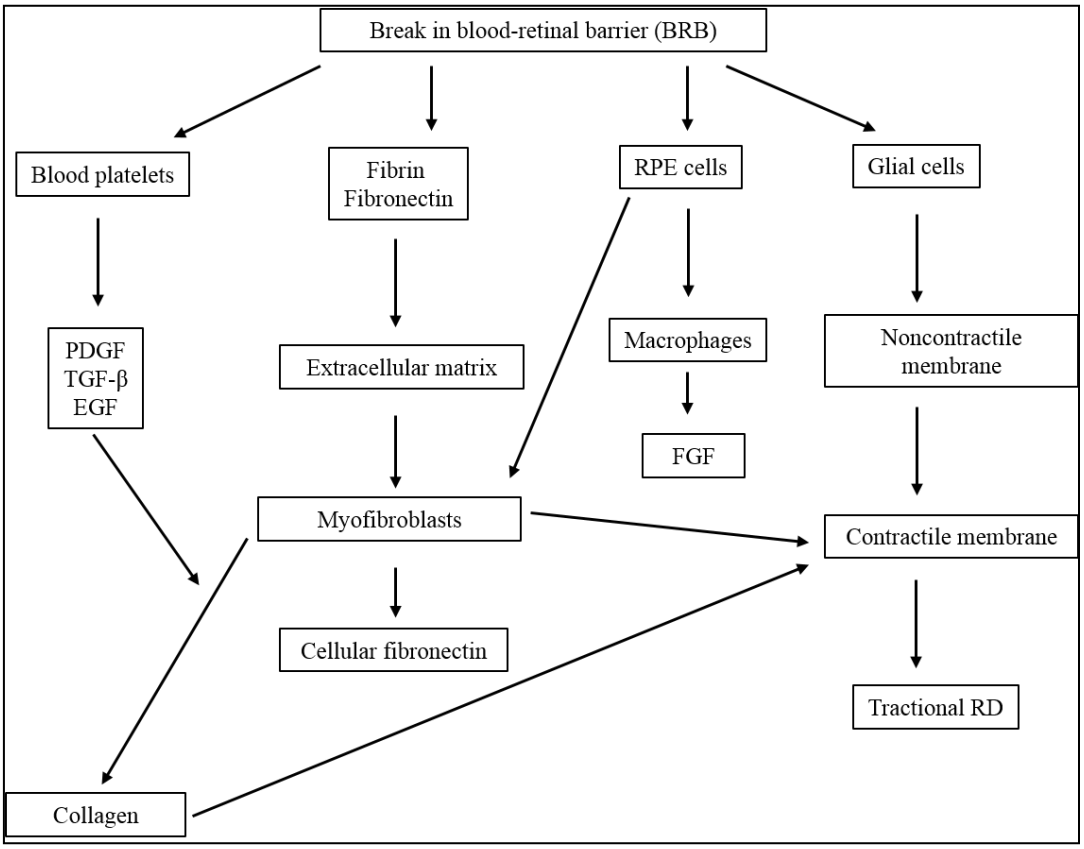

Figure 4. Pathogenesis of PVR (Adapted from Bozan et. al., 2004).

1.2. PVR Treatments

1.2.1 Surgery

Surgery is a standard treatment for PVR. Generally surgery has two main aims, these are sealing the retinal breaks and relieving the tractional forces while restoring the anatomy. Although conventional surgeries are satisfactory for light or moderate cases of PVR, advanced microsurgical techniques must be used in severe cases. These microsurgical techniques include peeling of epiretinal membranes, eliminating subretinal membranes and using some stabilizers (e.g perfluorocarbon liquids and silicone oil/gas) during surgery to facilitate epiretinal membrane removal. According to the literature, anatomic success of surgery is 60 – 80%, while the success of functional surgery is 30 – 40% with patients who have had anatomically successful surgery (Pastor et. al., 1998).

1.2.2 Medical Treatment as an Adjunctive Therapy

Medical tretment should be used jointly with surgery to minimize the risk of recurrence and improve poor functional results of surgery. A number of drugs have been tested in PVR treatment but there were some problems. For instance, free drugs have short half-lives and also show high toxicity (Bozan et. al., 2004). Therefore, using sustained release systems by encapsulating the drugs in carriers such as liposomes, nanoparticles or biodegradable microspheres has been accepted as an efficient approach. There are two main types of drugs used in PVR treatment; these are anti-inflammatory agents and antiproliferative agents (Sadaka et. al., 2012).

1.2.2.1 Anti-inflammatory Agents

Corticosteroids have been considered as anti-inflammatory agents due to their blood-retinal barrier stabilizing feature. They reduce the migration of inflammation mediators and also inhibit the proliferation of T-lymphocytes by stabilizing the blood-retinal barrier. Triamcinolone acetonide and dexamethasone are the most commonly used corticosteroids which modify cellular proliferation and inflammatory response. Although the benefical effect of corticosteroids has been known, there were conflicting reports in the literature. Animal studies showed that intravitreal triamcinolone acetonide injection achieved 64% reduction in retinal detachment (Hui et al.,1993). However clinical studies carried out by Faghihi et al. (2008) indicated that intravitreal injection of triamcinolone acetonide at the end of surgery had better outcomes in comparison to control patients who did not receive any intravitreal triamcinolone acetonide. In contrast, Jonas et. al. (2003) reported that there was no significant difference between the study group (triamcinolone acetonide injected at the end of surgery) and the control group. According to Pastor et al. (1998), corticosteroids were not suitable for postoperative PVR treatment because their most effective anti-inflammatory effects are seen in the early stages of inflammations.

1.2.2.2 Antiproliferative Agents

Proliferation of the cells (RPE cells, glial cells, fibroblasts and macrophages) is the key point in PVR progression, therefore, studies targeting inhibition of the

proliferation has been attempted by using antiproliferative agents such as 5-fluorouracil (5-FU), daunorubicin, doxorubicin, taxol, colchicine, retinoic acid and others. 5-FU has been the most commonly used agent *in vivo* PVR experiments and clinical trials. 5-FU suppresses DNA and RNA synthesis by inhibiting thymidine formation. It was found out that 5-FU does not show toxic effects at the required doses (Charteris, 1995). Animal studies indicated that 5-FU containing sustained release devices were highly effective in preventing PVR (Borhani et. al., 1995). Meanwhile, Pastor et. al. (1998) performed clinical trials and found that postoperative treatment of 5-FU (10 mg/day for 7 days) significantly reduced (36%) the recurrence of PVR.

Taxol and colchicine have also been studied for PVR treatment and it was found that they inhibit fibroblast proliferation and migration by stabilizing microtubulues and blocking G2 and M phases of the cell cycle (Sadaka et. al., 2012).

The effect of retinoids on PVR has been investigated and it was found that 13-cis retinoic acid has an antiproliferative effect on RPE cells. It was also shown that when 10 mg oral 13-cis retinoic acid was given to patients twice daily for 8 weeks after surgery, retinal attachment was successfully maintained and vision was improved (Chang et al., 2008). Likewise, cytotoxic effect of all-trans retinal, which is also vitamin A derivative, was shown in *in vitro* studies (Wielgus et. al., 2011). Also, Berckhuck et. al. (2013) showed that all-trans retinal has an antiproliferative effect on RPE cells and therefore have a potential as a new theurapeutic agent for PVR. According to Berchuck et al. (2013), all-trans retinal causes downregulation of membrane complement regulatory proteins (mCRPs) including CD46 and CD59 and so RPE become more susceptible to cell death.

1.2.2.2.1 Doxorubicin

Doxorubicin is an anthracycline group drug which was isolated from *Streptomyces peucetius.* It has been widely used in cancer treatments and has a great potential against both solid and liquid tumors. Although it has been using for many years, the molecular mechanism of action of doxorubicin has not been clarified yet. However, many mechanisms have been proposed and they include topoisomerase II poisoning, DNA adduct formation, oxidative stress and ceramide overproduction (Yang et. al.,

2014). Topoisomerase II poisoning and DNA adduct formation are the most commonly seen mechanisms of doxorubicin (Yang et al., 2014).

Topoisomerases are enzymes that are required for DNA replication and transcription. There are two isoforms of topoisomerases in humans: topoisomerase IIα and topoisomerase IIβ. During DNA replication and transcription, topoisomerase II basically binds the DNA supercoils, breaks the strand of the DNA duplex and reseals the break and causes the release of torsional stress (Pommier et. al., 2010). Also, topoisomerases are essential for decatenation of DNA during mitosis. In topoisomerase poisoning, doxorubicin causes stabilization the cleavage complex by trapping topoisomerase II at breakage sites and prevent resealing of DNA.

However, doxorubicin intercalates the DNA through GC base pairs because hydrogen bonds occur specifically between doxorubicin and guanine bases, and therefore, DNA adduct forms (Cutts et. al., 2005). It has been shown that the formation of DNA adducts causes cell death. The interaction between doxorubicin and DNA is shown in Figure 5.

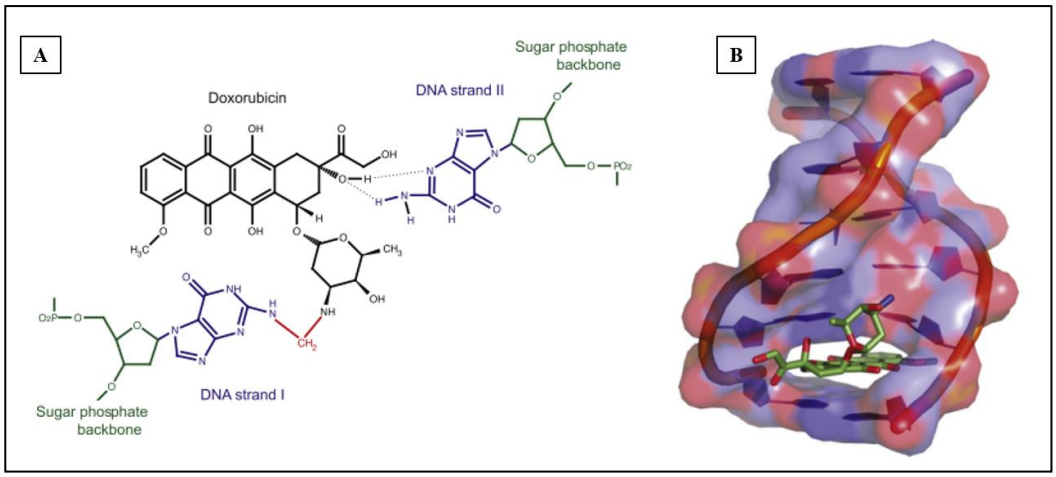

Figure 5. Illustration of DNA-doxorubicin complex. A) Covalent bond (shown in red) and hydrogen bond between doxorubicin and guanine, B) Intercalation of DNA by doxorubicin (Yang et al., 2014).

As seen in Figure 5, doxorubicin covalently binds the guanine base on one strand of DNA by cellular formaldehyde which occurs from lipids or spermine by free radical reactions. Also, hydrogen bond forms between doxorubicin and guanine on the other strand of DNA. Therefore, intercalating of DNA prevent the cell replication and transcription by doxorubicin which sits in the minor groove of DNA.

As mentioned above, the action mechanism of doxorubicin differs when different cell types or doses are used. In the literature, it is generally assumed that doxorubicin acts as a topoisomerase II poison in retinal pigment epithelial cells.

1.3 Drug Delivery Systems (DDS)

Drug delivery is a basic concept that implies administration of a therapeutic agent to the body in order to achieve treatment of diseases. However, conventional administration routes and techniques of drugs has many drawbacks. In a systemic application, the reaching of the drug to the desired tissues is a problem because of the many barriers in the body that need to be crossed. For instance, cellular membranes or intracellular compartments are among the main barriers. Drugs could loose efficacy during or after distribution. Besides uncontrolled levels of drugs and systemic distribution may lead to undesirable side effects on healthy tissues. Inability to maintain the drug concentrations is another problem of conventional treatments. Drug delivery systems (DDS) are designed to overcome these problems and to improve the efficacy and safety of drug, control the amount, rate, time and localization of the drug (Kagalkar et. al., 2013). Figure 6 shows that the difference between conventional therapy and DDS.

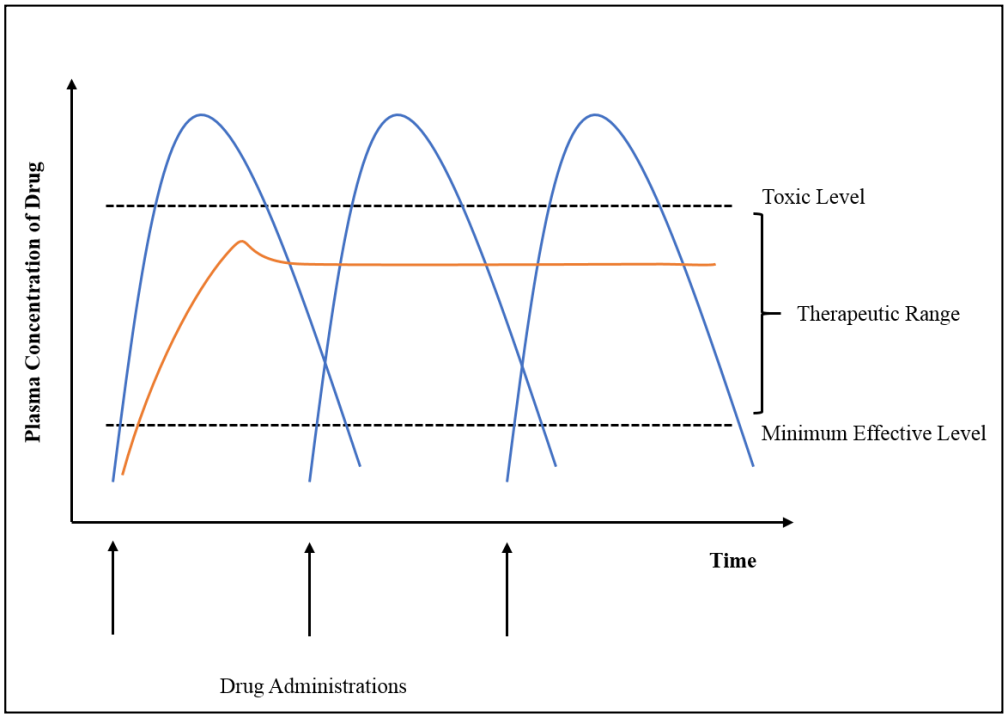

Figure 6. Drug levels in plasma for conventional oral drug delivery (blue plot) and DDS (orange plot).

In conventional drug delivery, after administration, plasma concentration of the drug rises, reaches a peak and then decreases below the minimum effective level. Therefore, repetitive administrations are required to keep the plasma concentration in the therapeutic range. In DDS, the goal is maintain the plasma concentration of the drug in the therapeutic range for an extended time, so that, an effective therapy could be achieved. Zero order kinetics (concentration not changing with time) is observed with perfect DDS, in other words the rate of drug release is independent of its concentration, and time while conventional treatment obeys First Order kinetics which is described as rate depending on drug concentration or drug release rate is decreased with time.

More sophisticated drug delivery systems could also be designed as targeted or responsive delivery systems to achive higher concentrations at the site of action or to achieve on-demand release.

1.3.1 Particulate DDS

Nanoscience and nanotechnology continues to receive increased attention in order to design more effective drug delivery systems. In accordance with this purpose, different types of particulate drug carriers have been developed by scientists using inorganic or metallic structures as well as synthetic or biological macromolecules or phospholipids. Although by definition nanoparticles have to be below 100 nm in diameter, particles to be used in drug delivery need to be larger than 100 nm for sufficient loading (De Jong et al., 2008). Sustained, controlled and targeted drug delivery could be achieved by modifiying surface characteristics of particles (Srikanth et. al., 2012). Particulate drug delivery systems have many advantages due to their small (micro and nano) size such as enhanced permeability through membranes. Stability of drug molecules could be improved by entrapping in particulate DDS.

Classification of nano and micro particles, their advantages and preparation methods are listed in Table 2.

Table 2. Types of nanoparticles used in DDS.

Drug Carrier System	Size Range	Advantages	Method of preparation
Microparticles, Natural or synthetic polymers, ceramics	< 200 µm	• Prolonged and targeted release	• Polymerization techniques, • Spray drying, • Solvent evaporation
Nanoparticles, Natural or synthetic polymers, ceramics	10-1000 nm	• Prolonged and targeted release	• Dispersion of preformed polymers, • Polymerization of monomers, • Ionic gelation of hydophilic polymers
Lipid nano and micro particles	50-1000 nm	• Avoidance of organic solvents, • Improved bioavailability	• High shear homogenization, • Ultrasonication, • Spray drying, • Solvent injection
Liposomes	25 nm-100 µm	• Highly bioavailable, • Ease of manufacturing, • Carry both hydrophilic and hydrophobic drugs	• Film hydration, • Reverse phase evaporation, • Dehydration-rehydration (DRV), • Membrane extrusion
Micelles	-	• Thermodynamic stability, • Suitable carrier for hydrophobic drugs	• Emulsion polymerization
Dendrimers	-	• High degree branching, • Globular architecture, • Well-defined molecular weight	• Divergent growth method, • Convergent growth method
Carbon nanotubes	0.7-1.5 nm: Single-walled carbon nanotubes, 2-50 nm: Multiwalled carbon nanotubes	• Water soluble, • Can be made biocompatible through chemical modification, • Multifunctionality	• Arc method, • Laser methods, • Chemical vapor deposition, • Ball milling

1.3.1.1 Liposomes

Liposomes are small bilayer vesicles which are composed of phospholipids (synthetic or natural) and cholesterol (Figure 7). They were first introduced by Bangham in 1965 for biological applications. Since then, liposomes have been widely used as models of biomembranes and also as carriers of bioactive agents.

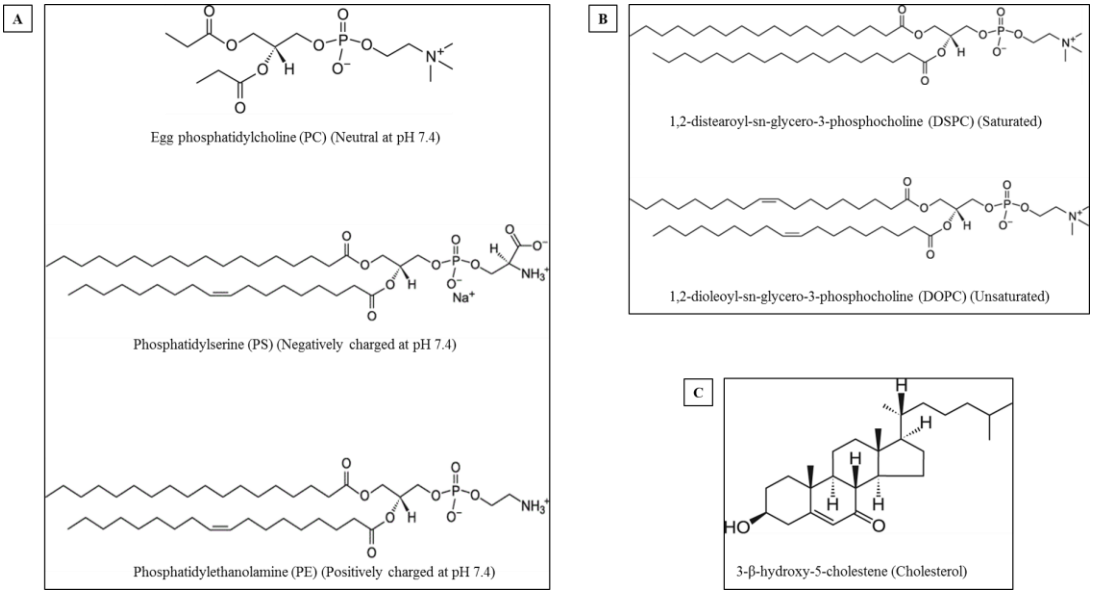

Figure 7. Main components of liposomes. A) Neutral and charged phospholipids, B) Saturated and unsaturated phospholipids, C) Cholesterol.

Liposomes have many advantages over other particulate systems, such as, they are highly biodegradable, non-toxic and non-immunogenic (Akbarzadeh et al., 2013). They can carry both hydrophilic and hydrophobic drug molecules in one particle due to their amphiphatic features (Figure 8A). One major disadvantage is that they are very labile; they are distrupted at such low temperatures as 40^{o}C, and they easily burst in a couple of days.

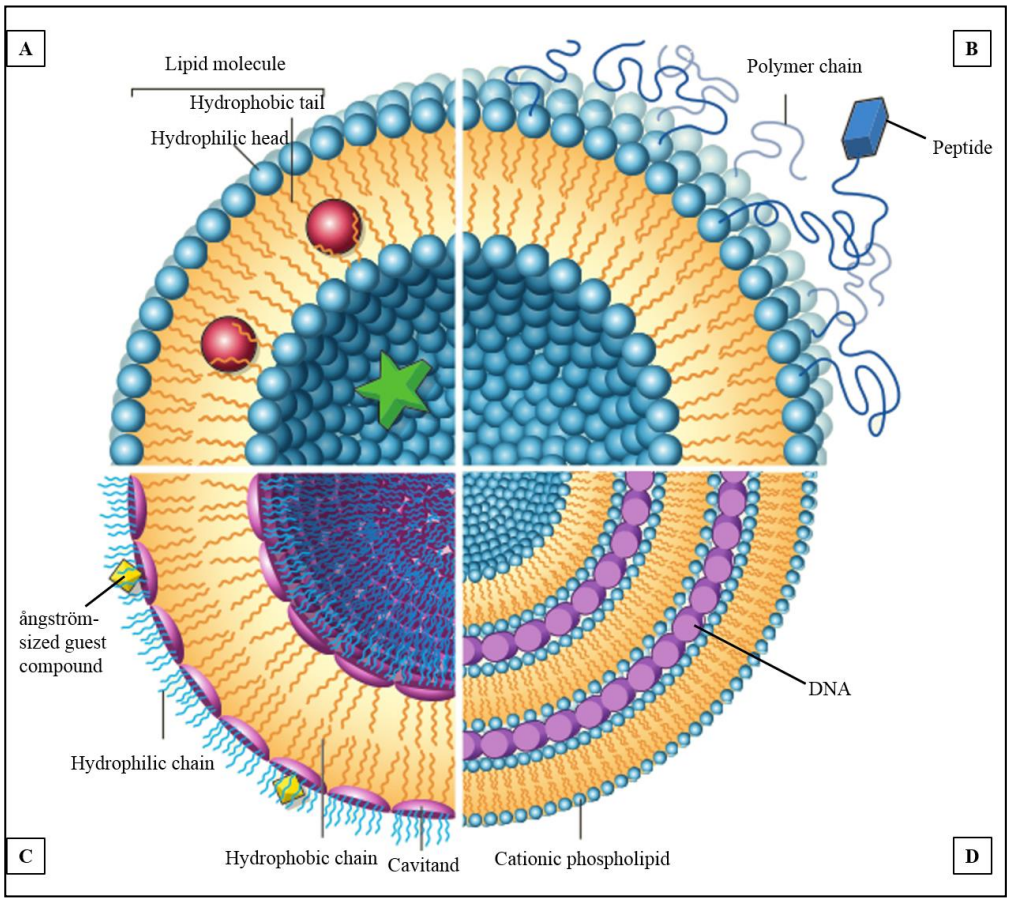

Figure 8. Schematic illustration of different types of liposomes. A) Conventional SUV liposome carries both hydrophilic (green star) and hydrophobic (red spheres) drug, B) PEGylated (blue curves) and peptide (blue rectangle) bound SUV liposome, C) Cavitand (purple hemisphere) containing SUV liposome, D) Cationic MLV liposome (Smolyanskaya et al., 2012).

When in human body, liposomes are cleared from the bloodstream by macrophages. "Stealth liposomes", liposomes which carry polyethylene glycol attached to their surfaces, were shown to overcome this problem by the hydrophilic layer attached onto their surfaces (Figure 8B). Surface of liposomes can be modified by using other molecules including peptides (Figure 8B). The peptides are selected to bind to specific receptors on cells and tissues, and targeted drug delivery could be achieved. The molecule to be attached can also be pore formers such as "cavitands", vase-shaped molecules, that can encapsulate ångström-sized guest compounds (yellow

diamonds in Figure 8C) (Kubitschke et. al., 2012) The charge of the liposomes can easily be defined by using a phospholipid with the right charge. An example of cationic liposome is seen in Figure 8D. Cationic liposomes are especially important because they can interact with negatively charged molecules such as the phosphate groups of DNA (purple rods in Figure 8D), makes a neutral complex and carries it with itself wherever it goes. This also helps stabilize the DNA and by neutralizing it, the DNA can penetrate the cells easier.

Pharmacokinetic features of liposomes are influenced by the membrane phospholipid composition, size, surface charge, method of preparation, dose and route of administration. There are four main types of liposomes when classified according to their size and lamellarity (Figure 9) :

- Multilamellar Vesicles (MLVs): They have multiple bilayers like an onion and their size is in the range of 1-5 μm. There is no need for the additional steps to produce these vesicles because they are formed spontaneously after the hydration step of normal liposomes preparation procedure. Hydrophilic drugs can be entrapped in the lamellar regions.
- Small Unilamellar Vesicles (SUVs): They have a single phosphlipid bilayer and their diameter changes between 20 and 200 nm.
- Large Unilamellar Vesicles (LUVs): They have also a single phosphlipid bilayer but their diameter changes between 200 nm and 1 μm.
- Multivesicular Vesicles (MVVs): They consist several small unilamellar vesicles in the aqueous core of one large unilamellar vesicle.

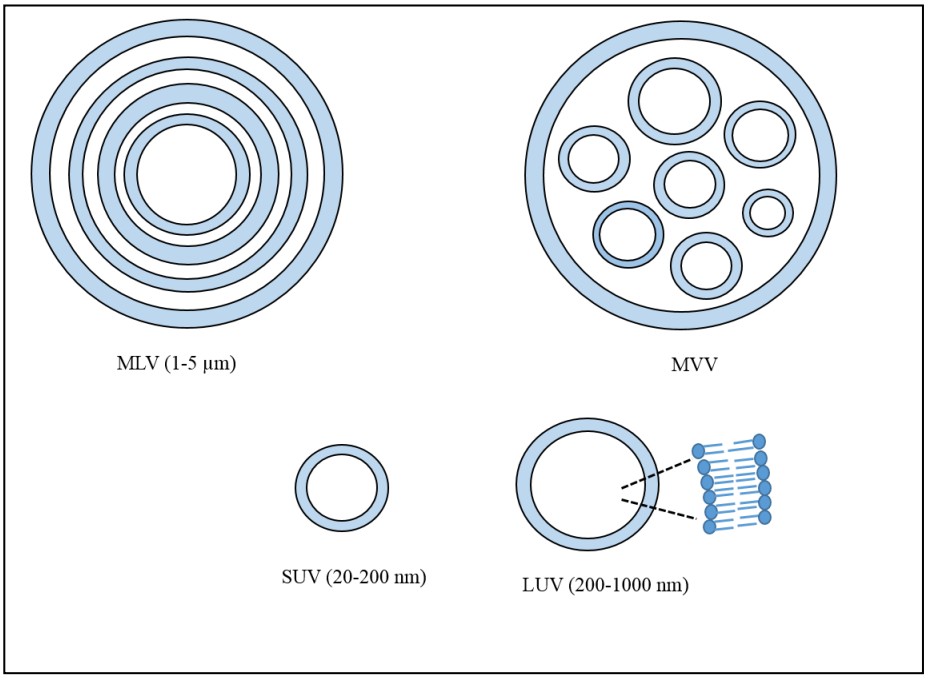

Figure 9. Various types of liposomes

Cholesterol is the second main component of liposome after the main ingredient, the phospholipids. Cholesterol gives rigidity and stability to the bilayers of the liposome. It is an amphiphatic molecule which has hydrophobic aliphatic chains and hydrophilic hydroxyl groups. Cirli et al. (2004) and others have reported that stability of liposomes increases with the cholesterol content, upto 30%, over this fraction the stability of the liposomes starts to decrease.

Liposomes have some disadvantages like having short shelf life and low stability. These lead to the leakage of drugs from liposomes or to their fusion of liposomes. High production cost is also an important problem (Dhandapani et. al., 2013). Although there are some problems in developing liposomal drug delivery systems with full therapeutic potential, researchers have developed methods to overcome these issues. There are many different methods of liposome preparation, but all share the same basic two stages: (1) Drying of phospholipids from organic solvents, and (2) Dispersion of the phospholipids in an aqueous medium. Liposomes are produced using different methods like film hydration, ether injection, dehydration-rehydration, reverse phase evaporation and membrane extrusion.

1.3.1.1.1 Dehydration-Rehydration (DRVs) Liposomes

Although there are many commercially available liposome formulations like Doxil®, Mycet®, DaunoXome® and AmbiSome®, instability of liposomes (oxidation or hydrolysis of phospholipids, drug leakage, liposome aggregation) is still an important issue for long term storage (Chen et. al., 2010). There are several methods developed to improve the stability of liposomes or increase the shelf life. Dehydration-rehydration method is one of these methods used for longer shelf life and improving encapsulation efficiency. One way is to prepare a powder version of the liposome which is rehydrated when needed. This is not increased stability but increased shelf life. The procedure basically consists of the dehydration of a suspension of empty SUVs and the drug solution by lyophilization. When needed the system is rehydrated and used. Zadi et. al., (2000) showed that the DRV method also leads to relatively high encapsulation efficiency of hydrophilic drugs due to the intimate contact between lipids and drug solutions. However, fusion of liposomes during freeze drying is an issue, but it can be prevented by using disaccharides such as sucrose to prevent aggregation. According to water replacement hypothesis, disaccharides maintain the head group spacing by reducing the van der Waals interactions between the acyl chains of phospholipids, and reduce the melting temperature (T_m) of the lipid membrane in its dry state. Therefore, the interactions between water and phopsolipids are decreased by using sugar until the rehydration step where the sugar and water replace.

1.4 Controlled and Responsive Delivery from Liposomes

Stimuli responsive delivery systems are designed to achieve high local doses at the site of action while reducing side effects. The release of the drugs is achieved upon the application of an environmental stimulus such as a change in temperature or pH, and exposure to light, which destabilizes the liposomes by a change in conformation or physical state of a sensitive agent in the liposome membrane structure.

1.4.1 Thermoresponsive liposomes

Thermoresponsive liposomes lose their integrity and release their content with application of heat to the target site to achieve targeted drug delivery. One of the

most often used method to develop thermoresponsive liposomes is based on destabilization of the membrane by increasing the local temperature above the phase transition temperature of at least one of the membrane components (Ganta et. al., 2008). Thermoresponsive liposomes are generally designed to be stable around physiological temperature (37^{o}C), but the membrane integrity of these liposomes is disrupted at a clinically achievable temperature such as 40 - 41^{o}C (Zhang et al., 2011). The second method used to develop thermoresponsive liposomes is the attachment of temperature sensitive polymers onto the liposomes and upon change of the temperature the liposomes are destabilized. Polymers which have low critical solution temperature (LCST) properties are used in these applications (Ta et. al., 2011). A third method involves the production of gas with heat and the gas destabilizes the membrane and cause release. Figure 10 presents the two examples of the thermoresponsive liposomes.

As seen in Figure 10A, a molecule called leucine zipper peptide was incorporated in liposome bilayer in folded conformation and above 43^{o}C it unfolds and expands, opens a channel in the membrane through which the drug, doxorubicin, is released. Thermoresponsive release of doxorubicin was also achieved with CO_2 gas that formed upon decomposition of encapsulated ammonium bicarbonate above 40^{o}C (Figure 10 B).

Although there are several successful studies with thermoresponsive liposomes, these systems have some challenges such as heat application cannot be tolerated if much higher temperatures than the physiological media is required. Besides, it is hard to treat distant metastasis with this method.

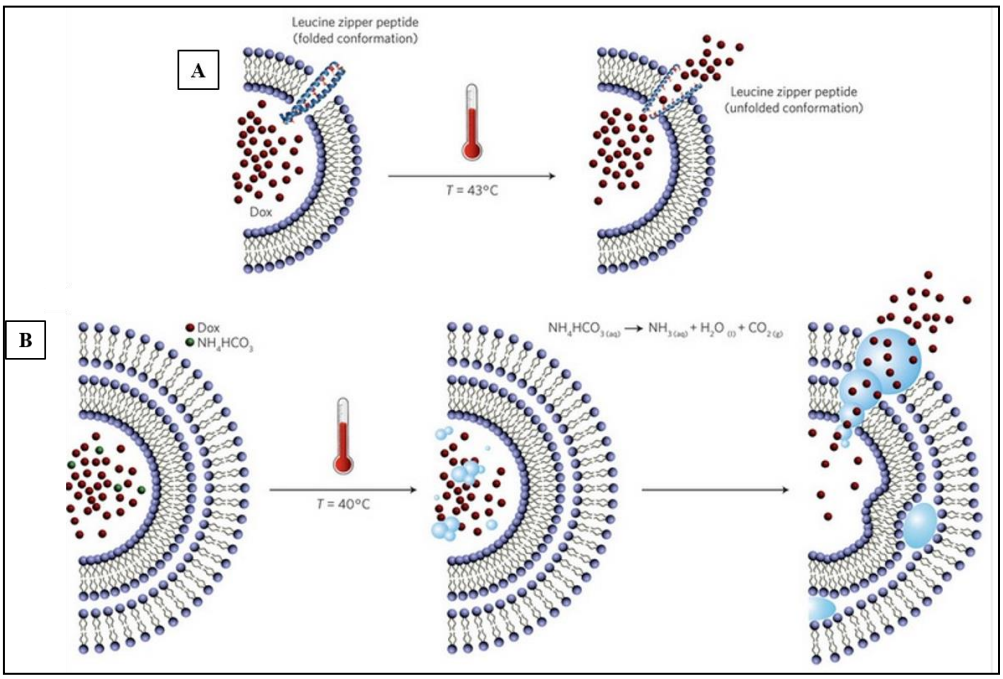

Figure 10. Thermoresponsive release of doxorubicin from: A) Leucine zipper peptide incorporated liposomes involves conformation change of a membrane component upon rising temperature, B) Ammonium bicarbonate containing liposomes in which CO_2 gas is produced upon rising temperature and that expands and enlarges the liposome (Mura et al., 2013).

1.4.2 pH Responsive Liposomes

pH responsive liposomes are stable at certain pHs and they are not when the pH is changed, and release their contents upon destabilization of the lipid membrane. Some pathological tissues (infected tissues and tumors) have a pH lower than the physiological pH (7.4) and when the liposome reaches this site, the membrane component gets ionized and this leads to the release of the drug (Ganta et al., 2008). The release of drug can be achieved either with phospholipids or with the pH sensitive polymers attached onto or encapsulated in the liposomes.

Phosphatidylethanolamine (PE) has been widely used phospholipid to prepare pH responsive liposomes. The primary amino head group of PE is protonated in the acidic enviroment and this changes its conformation in the membrane and leads to the release of the liposome content. There are also some limitations with these liposomes such as their instability and rapid clearance. These problems can be solved

by using lipid conjugates like PEG-PE or using phospholipids which have high transition temperatures such as 1,2-distearoyl-sn-glycero-3-phosphocholine (DSPC) or hydrogenated soya PC (HSPC) (Karanth et al., 2007).

1.4.3 Photoresponsive Liposomes

Drug delivery from photoresponsive liposomes is based on destabilization of phospholipid membrane by light induced isomerization, cleavage or polymerization of its components (Figure 11). Photoresponsive liposomes are generally designed with incorporation of light sensitive molecules into phospholipid bilayer. These photosensitive molecules change their conformation or chemistry upon exposure to light (UV or visible) with a specific wavelength and intensity. Retinoids, azobenzene moities, suprofen and photochromic phospholipid Bis-Azo PC are examples of light sensitive molecules (Leung et. al., 2012).

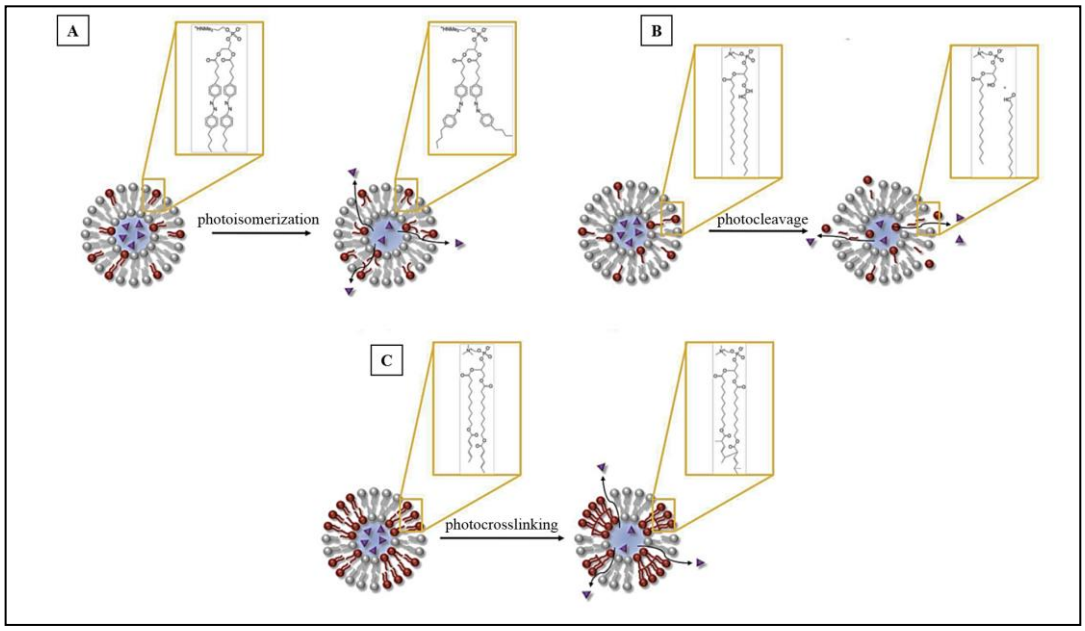

Figure 11. Photochemical release from liposomes. A) Photoisomerization, B) Photocleavage, C) Photocrosslinking (Adapted from Leung et. al., 2012).

In Figure 11A, it was showed that azobenzene incorporated into liposome bilayers and it changed its conformation from trans to cis form upon UV light exposure. Therefore, photoresponsive release of drug was achieved by destabilization of phospholipid membrane due to the steric effect cis form of azobenzene.

Photocleavage is another photochemical reaction that based on separation of the polar and nonpolar regions of an amphiphilic molecule (Figure 11B). Photocrosslinking is seen in Figure 11C where there is crosslinking of phospholipids upon UV irradiation and this leads to the destabilization of the phospholipid membrane and release of the content.

In the present study, all-trans retinal (ATR), a vitamin A derivative, was used as a light sensitive molecule to achieve photoresponsive release from liposomes. ATR changes its conformation upon UVA (365 nm) exposure to its 13-cis isomer which creates spaces in the membrane and leads to release of drugs (Gursel et al., 1995) (Figure 12).

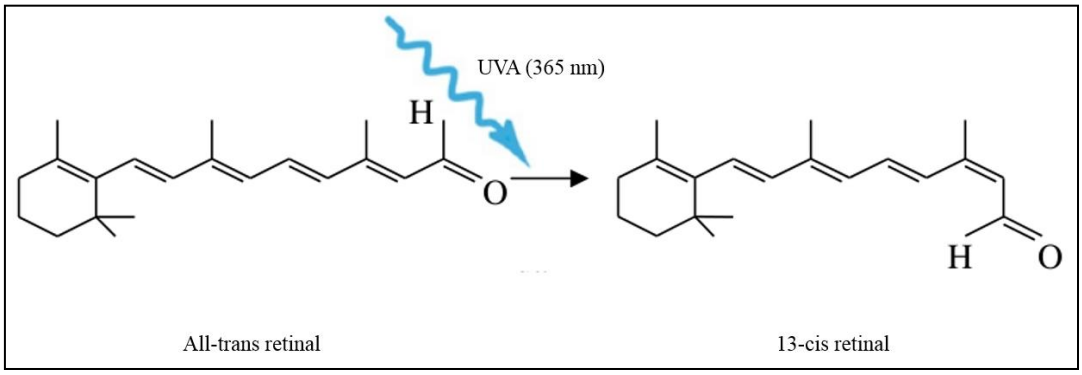

Figure 12. Photoisomerization reaction of all-trans retinal. The molecule goes from the "trans" state to a "cis" state upon exposure to UVA of 365 nm wavelength.

Although the majority of light-sensitive phospholipids are synthetic phospholipids, plasmalogen is an exception. Plasmalogen is a natural phospholipid which is found in tissues such as heart and brain and has characteristic vinyl ether linkages. It was proposed by Thompson et. al. (1996) that the reactivity of these vinyl ether linkages could be used to develop phototriggerable liposomes. Zn-phthalocyanine and bacteriochlorophyll-α were also used as photosensitizers which generate reactive oxygen species (ROS) and lead to destabilization of the liposomes through the reactivity of these molecules.

The clinical success of photoresponsive liposomes depends on many parameters like efficient drug loading, plasma stability before phototriggering, the applicability of the light source to the targeted tissues and use of patient-friendly light sources.

1.5 Aim and Novelty of the Study

The aim of this study was to develop photoresponsive liposomes for the treatment of ocular diseases that required frequent and continuous drug application. In this context, proliferative vitreoretinopathy (PVR) was selected as the model disease. PVR requires multiple intravitreal injections of the drug for a period longer than 4 weeks after surgery and this treatment causes several problems ranging from severe infections to cataract and also it is not a patient compliance method. Besides, many of antiproliferative agents that are used in the treatment of PVR have very short half lives (e.g 4-5 h) and they are highly toxic in their free form. Therefore, decreasing the toxicity and increasing the patient compliance were also the aims of this study. In order to achieve this, three different vitamin A derivatives (9-cis retinal, all-trans retinal and retinoic acid) were incorporated into phospholipid bilayers and their photosensitivies were studied. Liposomes with different compositions were prepared as given in Table 3 in section 2.2.1. Preliminary studies were carried out with calcein (CAL) as a fluorescent molecule serving as a model drug. After determination of the photoresponsive liposome composition, *in vitro* studies were performed to study the antiproliferative effects of all-trans retinal and doxorubicin on RPE/D407 cell line. Flow cytometry and confocal microscopy were performed to study the interactions between liposomes and cells.

In this study, for the first time in the literature, the effect of two different bioactive agents (all-trans retinal as membrane destabilizer and doxorubicin as antiproliferative agent) were studied simultaneously in the photoresponsive release of doxorubicin to influence RPE/D407 cell proliferation.

CHAPTER 2

MATERIALS AND METHODS

2.1 Materials

Lecithin (PC) (L-α-phosphatidylcholine from egg yolk) was purchased from Fluka (USA). Cholesterol (CHOL) (3-β-hydroxy-5-cholestene), calcein (CAL) (fluorescein-bis (methyl-iminodiacetic acid)) and chloroform ($CHCl_3$) were bought from Sigma-Aldrich (USA). All-trans retinal (ATR), 9-cis retinal (9CR), retinoic acid (RA) and Doxorubicin HCl were purchased from Sigma-Aldrich (USA). Triton X-100 was obtained from AppliChem (Germany). Potassium dihydrogen phosphate, dipotassium hydrogen phosphate and sucrose were purchased from Merck (Germany). Dialysis bag (Snake Skin pleated dialysis tubing, 10,000 MWCO) was obtained from Thermo Scientific (USA). Fetal Bovine Serum (FBS), Penicillin/Streptomycin (10,000 units/mL/10,000 μg/mL) and DMEM (Dulbecco's Modified Eagle Medium) high glucose modified was purchased from HyClone (USA). DMEM high glucose and Tyrpsin-EDTA (Ethylene Diamine Tetraacetic Acid) was obtained from Lonza (Sweden). Alamar blue® was obtained from Invtrogen Inc. (USA). Dimethyl sulfoxide (DMSO) was purchased from Sigma-Aldrich (USA). DRAQ5 was obtained from Abcam (USA).

2.2 Methods

2.2.1 Preparation of Standard and Modified Dehydration-Rehydration (DRV) Liposomes

Standard and modified liposomes were prepared with different compositions as listed in Table 3. Liposome components (PC, CHOL and vitamin A derivatives) were dissolved in chloroform and put into a round bottom flask (50 mL). The flask was

attached to the rotary vacuum evaporator (Bibby Sterilin, RE-100, UK), the temperature was adjusted to 39^{o}C, which is below the boiling temperature of the solvent and the rotation speed was set to 8-10 to obtain thin lipid film (TLF) after chloroform was removed completely. The flask was flushed with nitrogen gas to remove any residual chloroform. Liposomes were obtained spontaneously at the hydration step in which aqueous sucrose solution (sucrose:lipid, 1:1 (w/w), 2 mL) mixture was added onto thin lipid film and then agigated for 5 min on vortex (Heidolph Reax Top, Germany). At the end of the hydration step multilamellar vesicles (MLV) were obtained. Liposome suspension was sonicated for 10 min with 30 s intervals at 20 Watts to obtain small unilamellar vesicles (SUV). Liposome suspension was kept on ice during sonication to avoid oxidation of the lipids. At the end of this process, drug solution was added into the liposome solution and kept at -80^{o}C overnight before freeze dry. After freeze drying liposome powder was stored at -20^{o}C until its use.

Table 3. Compositions of liposome formulations.

Liposome Composition (Molar Ratio)		Code of Liposome Compositions	PC (mM)	CHOL (mM)	ATR (mM)	9CR (mM)	RA (mM)
Standard Liposomes	7:3	PC:CHOL 7:3	15.4	6.6	-	-	-
Modified (Vitamin-A Derivative Containing) Liposomes	7:3:1	PC:CHOL:ATR 7:3:1	15.4	6.6	2.2	-	-
		PC:CHOL:9CR 7:3:1	15.4	6.6	-	2.2	-
		PC:CHOL:RA 7:3:1	15.4	6.6	-	-	2.2
	7:1:3	PC:CHOL:ATR 7:1:3	15.4	2.2	6.6	-	-
		PC:CHOL:9CR 7:1:3	15.4	2.2	-	6.6	-
		PC:CHOL:RA 7:1:3	15.4	2.2	-	-	6.6

Before the use of liposomes, rehydration process was done. In this rehydration step, liposome powder was mixed with 200 µL distilled water and incubated at 50°C for 30 min. Then 400 µL phosphate buffer saline (PBS) (10 mM, pH 7.4) was added into the mixture and incubated with the same conditions. To separate liposomes from free unencapsulated drug, suspension was centrifuged at 22,000 g for 15 min at +4°C.

2.2.2 Characterization of Liposomes

For the prepared liposomes characterization studies which are size distribution, zeta potential, transmission electron microscopy (TEM) analysis and encapsulation

efficiency were done. Also, *in situ* releases of calcein and doxorubicin were studied to determine release profiles of the drugs from liposomes.

2.2.2.1 Size Distribution and Zeta Potential of Liposomes

After rehydration step, liposome suspension was centifuged to separate unencapsulated drug from liposomes. Then the precipitated liposome pellet was resuspended with 2 mL PBS (10 mM, pH 7.4) for determination of particle size and zeta potential of the liposomes (Malvern Zetasizer Nano ZS90 (UK)).

2.2.2.2 Transmission Electron Microscopy (TEM) Analysis

Liposomes were examined with TEM by negative staining with 2% uranyl acetate. TEM micrographs were obtained at 120 kV using a FEI Tecnai G^2 Spirit Bio (TWIN) microscope (USA, METU Central Lab).

2.2.2.3 Encapsulation Efficiency

Encapsulation efficiency (EE) was determined as the ratio of the amounts of the encapsulated drug in liposomes to the total input drug (Eq. I). Liposome suspensions were treated with Triton X-100 to distrupt liposomes and to detect encapsulated amount of the drugs. The fluorescence intensities of calcein and doxorubicin were detected by using spectrofluorometer at λ_{ex} 494 nm - λ_{em} 517 nm and λ_{ex} 480 nm - λ_{em} 590 nm, respectively. The amout of calcein and doxorubicin in liposomes were calculated by using the calibration curves (Appendix A and Appendix B).

$$EE = \frac{\text{The amount of drug in liposomes (mg)}}{\text{The amount of input drug (mg)}} X100 \quad \text{.....(I)}$$

2.2.2.4 *In Situ* Calcein Release from Nonresponsive and Photoresponsive Liposomes

In situ release studies of calcein were done for standard and modified liposomes. Half of the liposome suspension (1.5 mL) was kept in dark at room temperature and the other half was exposed to UVA (365 nm, 99 μWatts at a distance of 16 cm) for 45 minutes in a Petri plate. After that, the suspension was put in a dialysis bag (10,000 MWCO) and immersed into 15 mL phosphate buffer saline (PBS, 10 mM, pH 7.4). Release of calcein was performed at 100 rpm, 37ºC in an orbital shaker (Innova 4000 Incubator Shaker). Calcein amount released -was measured at λ_{ex} 494 nm, λ_{em} 517 nm by using a spectrofluorometer at predetermined time points.

2.2.2.5 *In Situ* Doxorubicin Release from Nonresponsive and Photoresponsive Liposomes

In situ doxorubicin release studies were done for PC:CHOL (7:3) and PC:CHOL:ATR (7:1:3) liposomes by the same technique (section 2.2.2.4).

2.2.3 *In Vitro* Studies

In vitro studies were performed by using RPE/D407 cell line. For this purpose, free doxorubicin, empty PC:CHOL:ATR (7:1:3) liposomes, and doxorubicin loaded PC:CHOL:ATR (7:1:3) liposomes were studied and Alamar Blue Cell Proliferation Assay was applied. Also cellular uptake of liposomal doxorubicin was analyzed with flow cytometry and confocal laser scanning microscopy (CLSM). RPE/D407 cells were incubated in DMEM high glucose medium with 10% Fetal Bovine Serum, 1% penicillin/streptomycin antibiotic and incubated at 37°C in humidified CO_2 incubator (5% CO_2).

2.2.3.1 Determination of RPE/D407 Cell Viability with Alamar Blue Cell Proliferation Assay

Alamar Blue Cell Proliferaton Assay was used to determine the number of live cells. The principle of the assay is a detectable color change with spectrophotometer due to

reduction of oxidized form of Alamar Blue by mitochondrial enzyme activity which is related to cell number.

In order to observe cell viability, RPE/D407 cells ($3x10^4$ cells/well) were seeded onto 24 well plates. After 4 h, drug formulations were added onto the cells. The proliferation profile of the cells were observed at 1, 2, 3 and 4 days of culture. At each time point, the wells were washed twice with sterile PBS (10 mM, pH 7.4) and incubated for 1 h with Alamar Blue solution (89% DMEM high modified colorless, 10% Alamar Blue and 1% penicillin/streptomycin) in CO_2 incubator. Then 200 μL of Alamar Blue solution was transferred into a 96 well plate, and the absorbances of all solutions were recorded at both 570 nm (λ_1) and 595 nm (λ_2) with an Elisa plate reader (Molecular Devices, USA). The percent reduction of the dye was calculated by the following equation:

$$\text{Percent Reduction} = \frac{[(\varepsilon_{ox})_{\lambda 2} \text{ x } A_{\lambda 1}] - [(\varepsilon_{ox})_{\lambda 1} \text{ x } A_{\lambda 2}]}{[(\varepsilon_{red})_{\lambda 1} \text{ x } A'_{\lambda 2}] - [(\varepsilon_{red})_{\lambda 2} \text{ x } A'_{\lambda 1}]} x100 \quad \text{.....(II)}$$

where,

$A_{\lambda 1}$= Absorbance of test well at λ_1= 570 nm

$A_{\lambda 2}$= Absorbance of test well at λ_2 = 595 nm

$A'_{\lambda 1}$= Observed absorbance of negative control well (blank) at λ_1= 570 nm

$A'_{\lambda 2}$= Observed absorbance of negative control well (blank) at λ_2 = 595 nm

$(\varepsilon_{ox})_{\lambda 2}$ = 117.216

$(\varepsilon_{red})_{\lambda 1}$ = 155.677

$(\varepsilon_{ox})_{\lambda 1}$ = 80.586

$(\varepsilon_{red})_{\lambda 2}$ = 14.652

Cell numbers were determined from a calibration curve constructed using the same procedure with known number of cells (Appendix C).

2.2.3.1.2 Effect of Free Doxorubicin on RPE/D407 Cell Viability

The effect of different concentrations of free doxorubicin on RPE/D407 cell viability was studied. Cells were seeded in 24 well plates ($3x10^4$ cells/well) and incubated in 1

mL DMEM high glucose medium containing 10% FBS and 1% penicillin/streptomycin for 4 h to achive cell attachment. After the cell attachment was completed, some medium was replaced with free doxorubicin to achieve different final concentrations of 0.01, 0.1, 1.0, 5.0 and 10.0 μg/mL. One of the control group had cells in doxorubicin free cell culture medium and the other one was added PBS (10 mM, pH 7.4) added cell culture medium at the highest volume of the drug. Alamar Blue Assay was performed at predetermined time points (Day 1, Day 2, Day 3 and Day 4).

2.2.3.1.3 Effect of PC:CHOL:ATR (7:1:3) Liposomes on RPE/D407 Cell Viability

The effect of different concentrations of PC:CHOL:ATR (7:1:3) liposomes on RPE/D407 cell viability was studied. PC:CHOL (7:3) and PC:CHOL:ATR (7:1:3) liposomes were prepared without loading any drugs (section 2.2.1). Cells were seeded into 24 well plates ($3x10^4$ cells/well) and incubated in DMEM high glucose medium for 4 h to achive cell attachment. After the cell attachment was completed, PC:CHOL (7:3) and PC:CHOL:ATR (7:1:3) liposomes were added at different concentrations (0.01, 0.1, 1.0, 5.0, 10.0 μg/mL). Control groups included only the cell culture medium and PBS (10 mM, pH 7.4) added cell culture medium. Alamar Blue Assay was performed at predetermined time points (Day1, Day 2, Day 3 and Day 4).

2.2.3.1.4 Doxorubicin Release from PC:CHOL:ATR (7:1:3) Liposomes

PC:CHOL:ATR (7:1:3) were prepared as mentioned in section 2.2.1. At the rehydration step, doxorubicin was encapsulated in the liposomes and the resultant liposomes were separated from unentrapped doxorubicin by centrifugation as explained in section 2.2.1. Half of the liposome suspension was kept in dark at room temperature and the other half of the liposome suspension was exposed to UVA (365 nm, 99 μWatts at a distance of 16 cm) for 45 min before they were introduced into the cell culture medium. Then liposome suspensions were added at a final concentrations of 0.01, 0.1, 1.0, 5.0, 10.0 μg/mL. Control groups were the same with

section 2.2.3.1.2. Alamar Blue Assay was performed at predetermined time points (Day1, Day 2, Day 3 and Day 4).

2.2.3.2 Cellular Uptake

2.2.3.2.1 Flow Cytometry Analysis

In order to study the interaction between liposomes and cells, RPE/D407 cells were seeded into 6 well plates ($3x10^5$ cells/well) and incubated in DMEM high glucose medium for 4 h to achive cell attachment. After the cell attachment was completed, empty PC:CHOL:ATR (7:1:3) liposomes, free doxorubicin, doxorubicin loaded UVA unexposed PC:CHOL:ATR (7:1:3) liposomes and UVA exposed PC:CHOL:ATR (7:1:3) liposomes were introduced into the cell culture with the same concentration as 1 μg/mL. Then, samples were further incubated for 4 h. Control group cells in the culture medium did not have any drug or liposomes. At the end of the incubation period, cells were detached from 6 well plates with tyrpsin (0.05%) and transferred into Eppendorf and washed with PBS (10 mM, pH 7.4). After that, cells were fixed with paraformaldehyde (1 mL, 4%, 15 min), and then treated with DRAQ5 for 30 min at the room temperature for nuclei staining and also washed with PBS (10 mM, pH 7.4) twice to discard excess dye. The fluorescence intensities were examined with flow cytometer (Accuri C6, USA). DRAQ5 was excited with 640 nm laser and detected with FL4A (675 ± 25 nm) detector. Also, all-trans retinal in PC:CHOL:ATR (7:1:3) liposomes and doxorubicin were excited with 488 nm laser and detected with FL2A (585 ± 40 nm) detector.

2.2.3.2.2 Confocal Laser Scanning Microscopy (CLSM) Analysis

Interaction between liposomes and cells was studied with confocal laser scanning microscopy (CLSM, Leica DM2500, Germany). RPE/D407 cells were seeded onto cover slips in each well of 6 well plate ($3x10^4$ cells/well) and incubated in DMEM high glucose medium for 4 h to achive cell attachment on the cover slips. After the cell attachment was completed, empty PC:CHOL:ATR (7:1:3) liposomes, free doxorubicin, doxorubicin loaded UVA unexposed and UVA exposed

PC:CHOL:ATR (7:1:3) liposomes were introduced into the cell culture with the same concentration (1µg/mL). Then, cells were further incubated for 4 h. Control group included only the cell culture medium. Cells were fixed with paraformaldehyde (1 mL, 4%, 15 min), and then treated with DRAQ5 for 15 min in CO_2 incubator (37ºC, 5% CO_2) for nuclei staining and washed with PBS (10 mM, pH 7.4) twice to discard excess dye. Specimens were excited with 635 nm laser for DRAQ5 and 488 nm laser for doxorubicin and all-trans retinal in PC:CHOL:ATR (7:1:3) liposomes.

2.2.4 Statistical Analysis

All of the characterization and *in vitro* studies were performed in triplicates. 1-tail Student's t-test was used to determine significant differences between mean values in control and test groups. $p \leq 0.05$ values were considered significantly different.

CHAPTER 3

RESULTS AND DISCUSSION

3.1 Characterization of Liposomes

Several characterization tests were carried out to determine the properties of liposomes. For this purpose, size distribution and zeta potential analysis, TEM analysis, encapsulation efficiency determination and *in situ* release profile studies were performed.

3.1.1 Size Distribution and Zeta Potential of Liposomes

Particle size and zeta potential analysis of PC:CHOL (7:3) and PC:CHOL:ATR (7:1:3) liposomes were carried out using Malvern Zetasizer Nano ZS90 (UK). Size and zeta potential of liposomes are shown in Table 4. Additionally, all of liposome types were analyzed with transmission electron microscopy (TEM) by using uranyl acetate for negative staining (Figure 13).

Table 4. Particle size and zeta potential analysis of different liposome formulations.

Liposome Composition	Particle Size (nm)	Zeta Potential (mV)
PC:CHOL (7:3)	137 ± 18	-44.56 ± 1.27
PC:CHOL:ATR (7:1:3)	918 ± 20	-43.20 ± 4.46

It was observed that PC:CHOL (7:3) liposomes were in the range of SUV as a monodisperse (PDI=0.436) population. A slight increase in particle size was expected with incorporation of all-trans retinal into the bilayer, but there was a large difference between PC:CHOL (7:3) and PC:CHOL:ATR (7:1:3) liposomes (Table 4).

However, according to TEM micrographs (Figures 13A and 13B), addition of all-trans retinal into the liposome membrane structure did not result in a large increase in particle size. It can be explained as; the particle sizer gives an average value depending on the diffraction of light, where in case of TEM, the sizes were measured from the images. It is thought that TEM results are closer to true value by considering the probability of diffraction due to fluorescence of ATR.

As presented in Table 4, zeta potentials of PC:CHOL (7:3) and PC:CHOL:ATR (7:1:3) liposomes were close to each other and distinctly negative (ca. -44 mV). In fact, a neutral zeta potential was expected for both PC:CHOL (7:3) and PC:CHOL:ATR (7:1:3) liposomes because of the neutral nature of their components at pH 7.4. Phosphatidylcholine is a zwitterionic molecule which has anionic phosphate group and a cationic amine group so it should normally be neutral but it was reported that natural egg phosphatidylcholine might have a small amount of negatively charged lipid and this could contribute to the anionic nature (Er, 2005).

Figure 13 shows that all the different liposome types were spherical and had unilamellar structure as expected. Some specks seen in the micrographs are probably due to crystals of PBS salts and residual uranyl acetate, and should be considered artifacts. As a result of particle size and TEM analysis, it was concluded that liposomes did not aggregate as a result of sucrose used in the dehydration step. Sucrose is known to prevent fusion of liposomes during freeze drying (Hincha et al., 2002). It was also found that disaccharides such as sucrose were more effective in the stabilization of liposomes than mono or polysaccharides (Kawano et al., 2003). Zadi et al. (2000) also showed that sucrose to lipid ratio was an important factor that effects the encapsulation efficiency. They reported that when sucrose fraction is high (e.g sucrose:lipid, 5:1 w/w) the encapsulation efficiency is decreased significantly. In this study a low ratio of sucrose to lipid (1:1 w/w) was used since it was reported that the ratio was enough to prevent the fusion of liposomes without any adverse effects on their encapsulation efficiency (Mugabe et al., 2006).

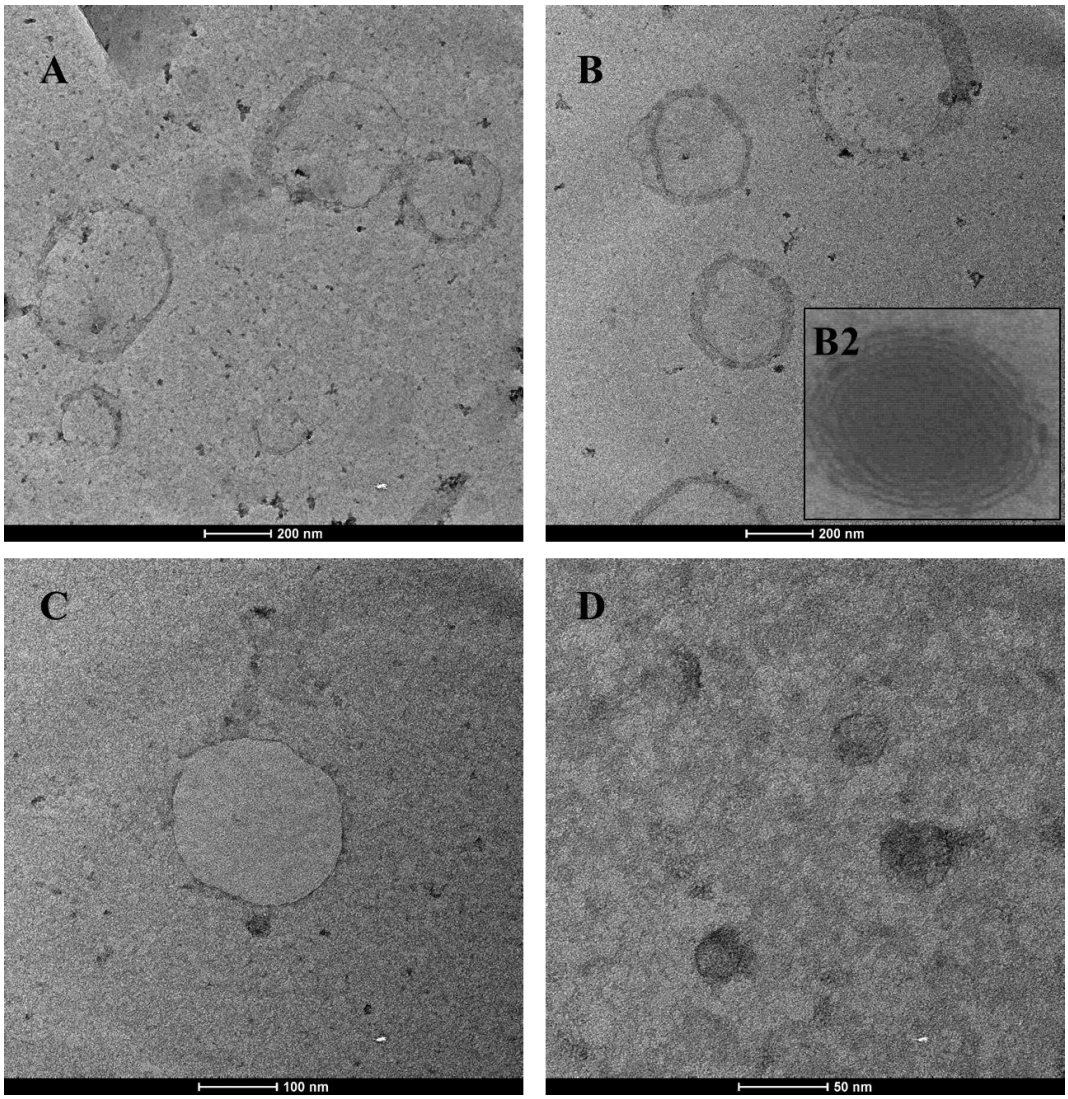

Figure 13. TEM micrographs of liposomes. A) PC:CHOL (7:3) empty, B) PC:CHOL:ATR (7:1:3) empty, B2) PC:CHOL MLV (Manca et. al., 2012) C) Doxorubicin loaded, UVA unexposed PC:CHOL:ATR (7:1:3) and D) Doxorubicin loaded, UVA exposed PC:CHOL:ATR (7:1:3) liposomes.

3.1.2 Encapsulation Efficiency

In order to study the effect of vitamin A derivatives, 9-cis retinal (9CR), all-trans retinal (ATR) and retinoic acid (RA), on the encapsulation efficiency of the liposomes, 7 different liposome formulations were prepared with the use of the same initial amount of calcein (4 μM) as given in Table 3. Figure 14 shows encapsulation efficiencies of different liposome formulations.

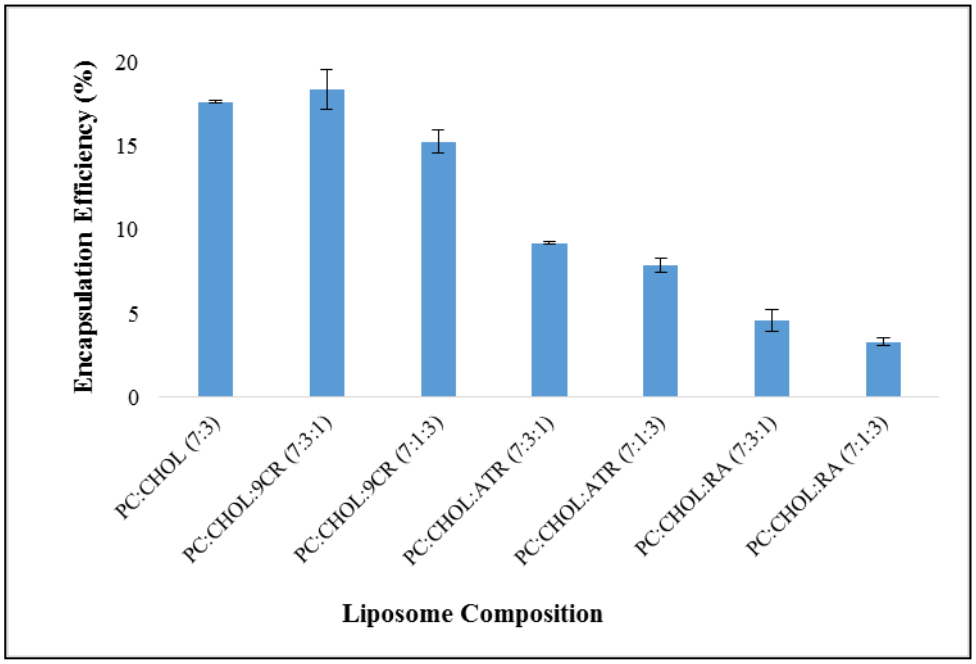

Figure 14. Encapsulation efficiencies of different liposome formulations. PC: Phosphotidylcholine; CHOL: Cholesterol; 9CR: 9-cis Retinal; ATR: All-trans Retinal; RA: Retinoic Acid.

As seen in Figure 14, encapsulation efficiency of calcein decreases upon addition of vitamin A derivatives into the bilayer of each liposome which indicates 9-cis retinal, all-trans retinal and retinoic acid lead to decrease the membrane permeability. In this context, it could be assumed that these vitamin A derivatives have cholesterol like effect on the membrane rigidity, for instance, when they exist in large amounts in the bilayer, conformational order and the stiffness of the membrane increases while the permeability of the membrane decreases (Raffy and Teissié, 1999). Tseng et. al. (2007) showed that increasing membrane ridity of liposomes with addition of cholesterol in liposome with transition temperature and deformability studies.

Decrease in membrane permeability is very important for encapsulation efficiency because in the DRV method, drugs are encapsulated into liposomes after the initial liposome formation step is completed. Additionally, it is seen that the large entrapment efficiency increase of the liposomes for calcein (3.29 to 18.38%) was achieved by using DRV method during liposome preparation. According to Zadi et al. (2000), in the DRV method, drug molecules contact the lipids intimately, so that relatively large amounts of drugs can be entrapped in the aqueous phase of the liposomes.

3.1.3 *In Situ* Release of Calcein

Release studies were performed for PC:CHOL (7:3) and the modified liposomes in order to study the effect of UVA on the release of calcein. In accordance with this purpose, half the liposome suspension was kept in dark at room temperature unexposed (-UVA) and the other half was exposed to UVA (+UVA) for 45 min (section 2.2.2.4). The release profiles of calcein from PC:CHOL (7:3) and modified liposomes were studied by determining the amount of calcein in the release medium (PBS 10 mM, pH 7.4) using spectrofluorometry at λ_{ex} 494 nm and λ_{em} 517 nm (Figure 15). The release of calcein percent from unexposed PC:CHOL (7:3) liposomes served as a blank (zero percent) to calculate the relative release of calcein from the other, modified, liposome compositions.

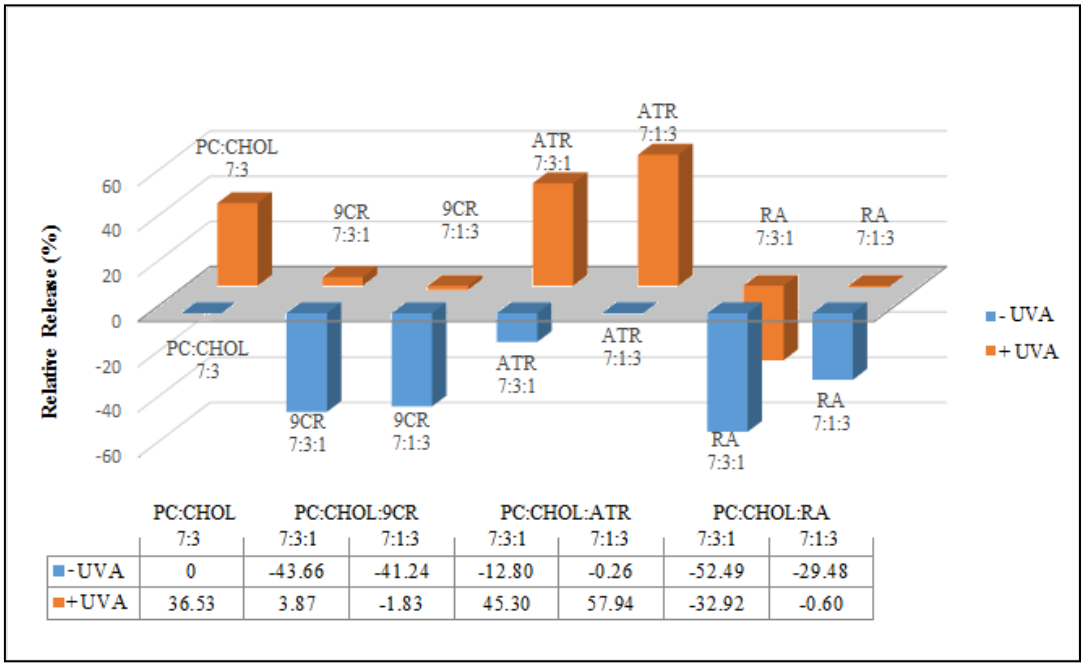

	PC:CHOL	PC:CHOL:9CR		PC:CHOL:ATR		PC:CHOL:RA	
	7:3	7:3:1	7:1:3	7:3:1	7:1:3	7:3:1	7:1:3
-UVA	0	-43.66	-41.24	-12.80	-0.26	-52.49	-29.48
+UVA	36.53	3.87	-1.83	45.30	57.94	-32.92	-0.60

Figure 15. Relative release of calcein from different liposome formulations within 96 h. PC: Phosphotidylcholine; CHOL: Cholesterol; 9CR: 9-cis Retinal; ATR: All-trans Retinal; RA: Retinoic Acid.

When the release of calcein from UVA unexposed PC:CHOL (7:3) liposomes is taken as the balnk (zero percent), the effect of UVA on the release behavior could be interpreted as positive or negative. In Figure 15, two main groups are observed: Relative release of calcein from -UVA liposomes (unexposed) (below the zero plane) and +UVA (exposed) liposomes (above the zero plane).

The results of these release studies show that the relative release of calcein from UVA unexposed modified liposomes, relative to the unexposed original, had a negative value for all liposome formulations indicating that each vitamin A derivative (9-cis retinal, all-trans retinal and retinoic acid) incorporated in the liposomal membrane increased the stability or rigidity of liposomes to some extent. However, UVA exposure led to a release of around 35% of calcein from PC:CHOL (7:3) liposomes which did not contain any vitamin A derivative. This is possibly due to lipid peroxidation reactions (Cirli et al., 2004). It was, therefore, expected that a release response higher than 35% was needed to indicate photosensitivity. In Figure 15, this can be seen in the ATR carrying liposomes, PC:CHOL:ATR (7:3:1) and

PC:CHOL:ATR (7:1:3): This means that photosensitivity is observed in the presence of ATR. Gursel et al. (1995) showed the conversion of ATR to its 13-cis isomer and this isomer distrupted the stability of the liposomal membrane.

The time dependent release of calcein from PC:CHOL (7:3) and PC:CHOL:ATR (7:1:3) liposomes are presented in Figure 16.

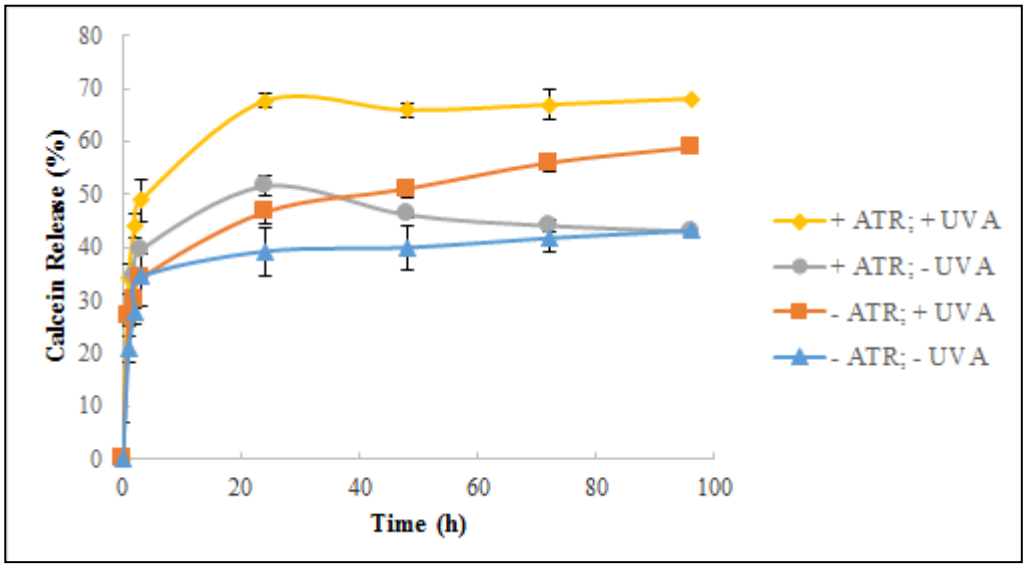

Figure 16. Influence of ATR presence and exposure to UVA on calcein release from the liposomes.

In Figure 16, it is seen that during a burst in the first 24 h, 35 to 65% of the calcein content is released; then the release rate decreased, leading to biphasic release profiles. There was no significant difference between the release rates from the UVA unexposed liposomes. The ratio of PC:CHOL is known to have an important effect on the initial release rate, and introduction of more cholesterol decreases the release rate due to the positive effect of cholesterol on the stability of lipid bilayers (Nounou et al., 2006). Thus, all-trans retinal appears to have a cholesterol like effect on the membrane stability.

In order to analyze the release kinetics of calcein from liposomes, a calcein release (%) versus square root time ($h^{1/2}$) graph was plotted for the first 24 h (Figure 17).

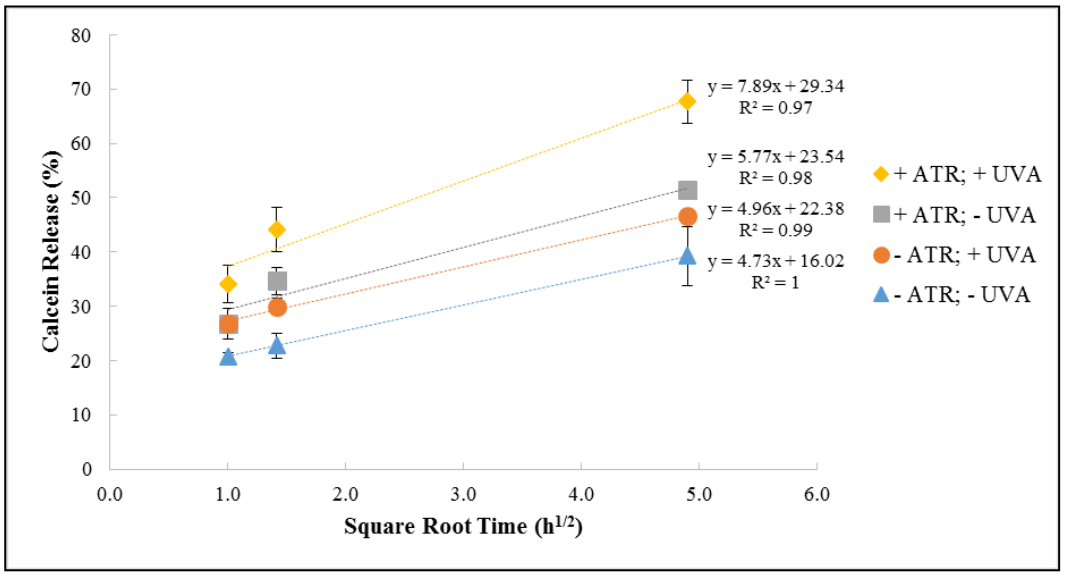

Figure 17. Release kinetics of calcein plotted according to Higuchi equation.

This would also check whether the release kinetics fitted that of the Higuchi equation ($M_t/M_\infty = k_H.t^{1/2}$). In the equation; M_∞ is the amount of the drug released at infinity (∞), t is the time (h) and k_H is the rate constant of the release. It is observed that all the release data fits the Higuchi equation indicating a diffusion based release (Figure 17 and Table 5).

Release rate coefficients (k_H) were calculated from the slopes of the release kinetics graph (Table 5). There is a significant difference (T-test, $p<0.005$) between the release rates of UVA exposed PC:CHOL (7:3) liposomes and PC:CHOL:ATR (7:1:3).

Table 5. Release rate coefficients (k_H) obtained using the Higuchi equation using release of Calcein from PC:CHOL (7:3) and PC:CHOL:ATR (7:1:3) liposomes.

Liposome Composition	k_H ($h^{-1/2}$)	
	UVA Unexposed (-UVA)	UVA Exposed (+UVA)
PC:CHOL (7:3)	4.73 ± 2.85	4.96 ± 1.68
PC:CHOL:ATR (7:1:3)	5.77 ± 1.31	7.89 ± 3.84

It was, therefore, decided to use PC:CHOL:ATR (7:1:3) liposomes in the *in vitro* studies due to their higher photoresponsiveness.

3.1.4 *In Situ* Release of Doxorubicin from PC:CHOL:ATR (7:1:3) Liposomes

In order to study the *in situ* release of doxorubicin, PC:CHOL:ATR (7:1:3) liposomes were prepared with 2 mg/mL initial concentration of doxorubicin. The encapsulation efficiency of the liposomes for doxorubicin was around 9.40 ± 0.80%. Release studies were carried out using the same technique described in section 2.2.2.5 for both UVA unexposed (-UVA) and UVA exposed (+UVA) conditions. The time dependent release of doxorubicin from PC:CHOL:ATR (7:1:3) liposomes is presented in Figure 18.

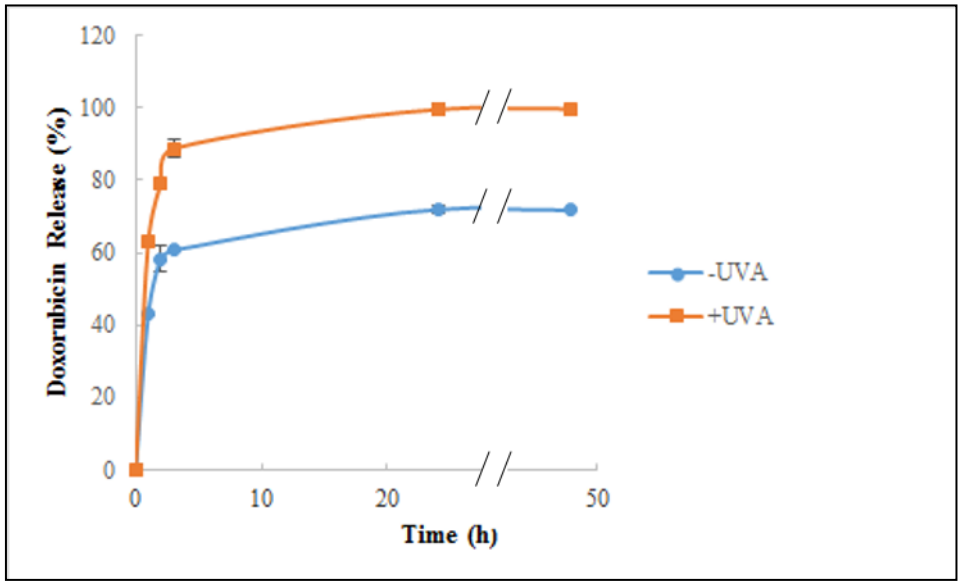

Figure 18. Influence of exposure to UVA on the release of doxorubicin release from PC:CHOL:ATR (7:1:3) liposomes.

It is observed that 60 and 88% of doxorubicin was released in the initial 3 h, for –UVA and +UVA liposomes, respectively, and then the release rate decreased (Figure 18). The initial burst effect observed in the release profiles could probably be due to the hydrophilic nature and low molecular weight of doxorubicin (Nouno et al., 2006). According to Johnston et. al. (2008), first burst release of doxorubicin could result from the high drug to lipid ratio which leads to a high concentration gradient and an increase in the release rate, but 10% encapsulation efficiency is not likely to create such a high gradient.

The release profiles were plotted according to Higuchi equation and it was found that the release data fitted the Higuchi relation for both UVA unexposed and UVA exposed liposomes (Figure 19).

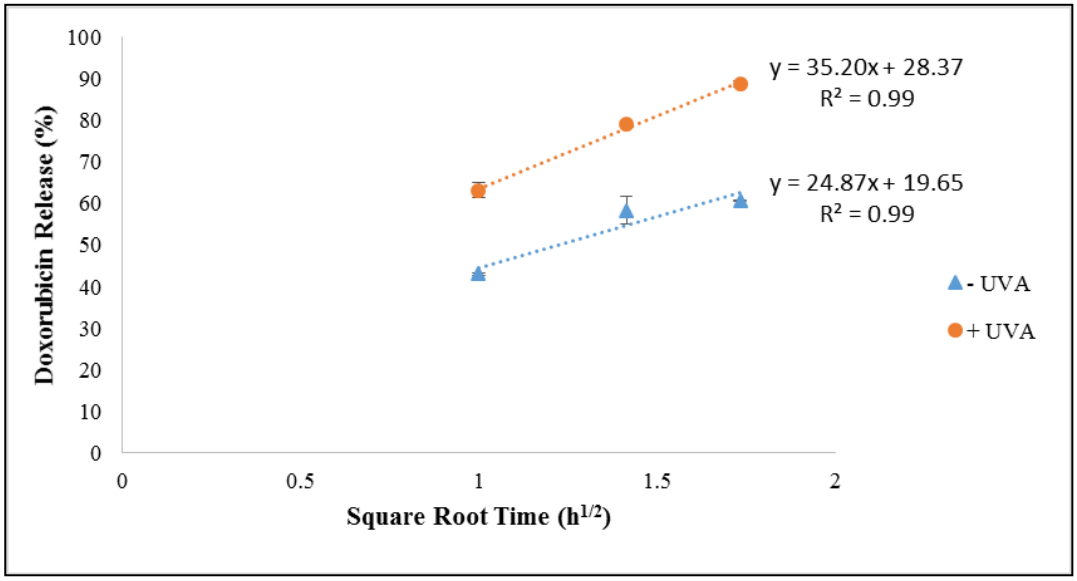

Figure 19. Release kinetics of doxorubicin from UVA unexposed (-UVA) and UVA exposed (+UVA) PC:CHOL:ATR (7:1:3) liposomes.

Release rate coefficients (k_H) for UVA unexposed and UVA exposed PC:CHOL:ATR (7:1:3) liposomes were calculated as 24.87 ± 0.86 and 35.20 ± 1.86, respectively, showing a significant increase (T-test, $p<0.005$) with the addition of ATR, also confirming the results obtained for calcein release.

3.2 *In vitro* Studies

In vitro studies were performed using retinal pigment epithelial cells to study the effect of free doxorubicin, liposome entrapped doxorubicin, and empty liposomes.

3.2.1 Effect of Free Doxorubicin on RPE/D407 Cell Proliferation

In order to determine the effect of free doxorubicin on RPE/D407 cells, final concentrations of 0.01, 0.1, 1.0, 5.0 and 10.0 µg/mL of free doxorubicin were prepared in the cell culture medium. The cell numbers were determined with Alamar Blue Cell Proliferation Assay at predetermined time points as mentioned in section 2.2.3.1.2 (Figure 20).

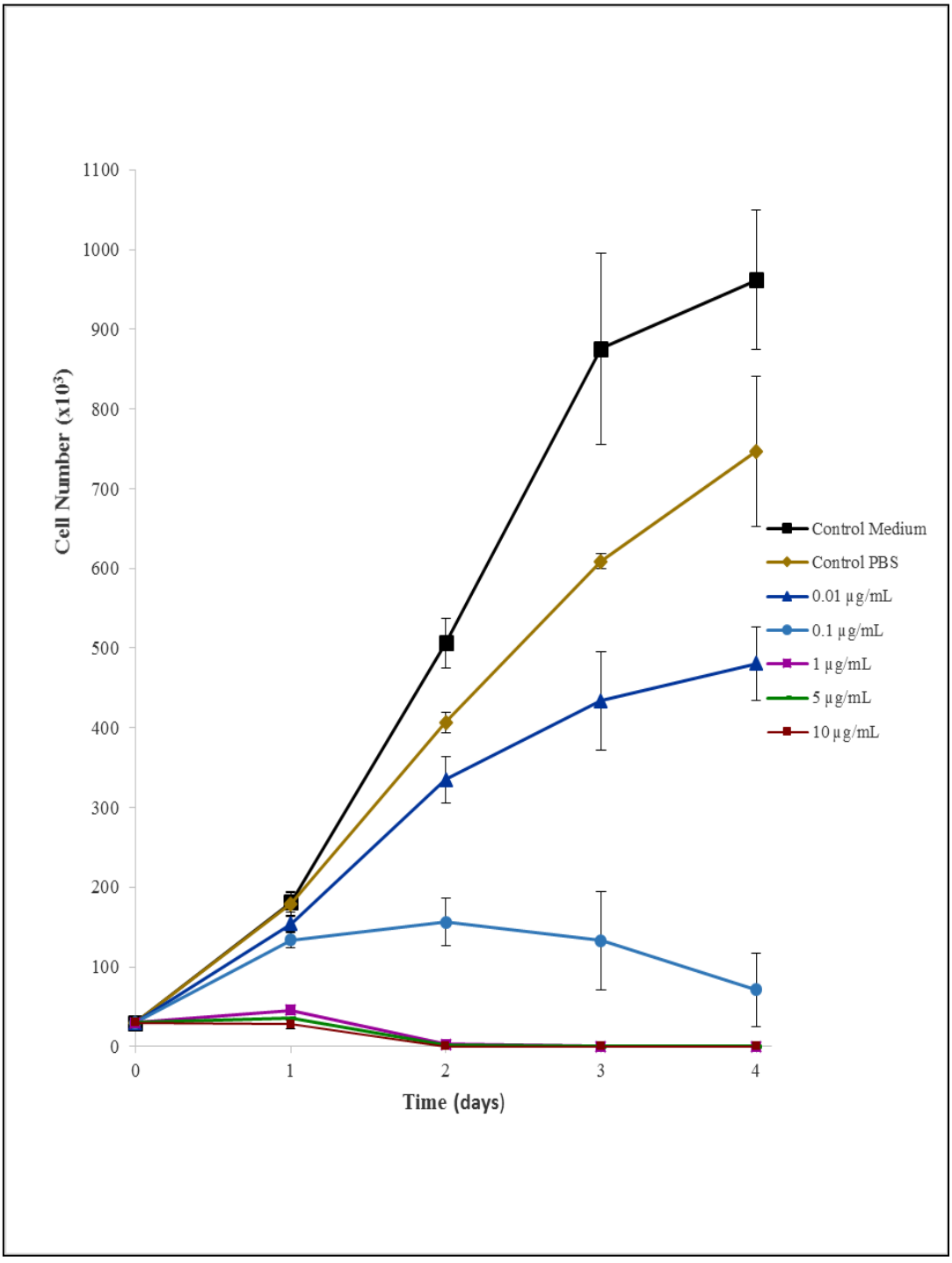

Figure 20. The effect of concentrations of free doxorubicin on RPE/D407 cells ($3x10^4$ cells/well). Control Medium: RPE/D407 cells incubated in the cell culture medium without any doxorubicin; Control PBS: RPE/D407 cells incubated in the PBS added cell culture medium at the highest volume of doxorubicin

Doxorubicin is a topoisomerase II inhibitor which intercalates the bases in DNA and creates an antiproliferative effect on RPE/D407 cells (Kuo et al., 2007). The results presented in Figure 20 support this antiproliferative effect of doxorubicin in a concentration dependent manner. As the concentration increased from 0.01 to 1 µg/mL the antiproliferative effect increased. There was, however, no significant difference in the doxorubicin concentration range 1-10 µg/mL. Dose-Response curves were plotted based on the data obtained on Days 1 and 4 (Figure 21). In this test the negative control was the drug-free test medium and positive control (100% effect) was no cell survival.

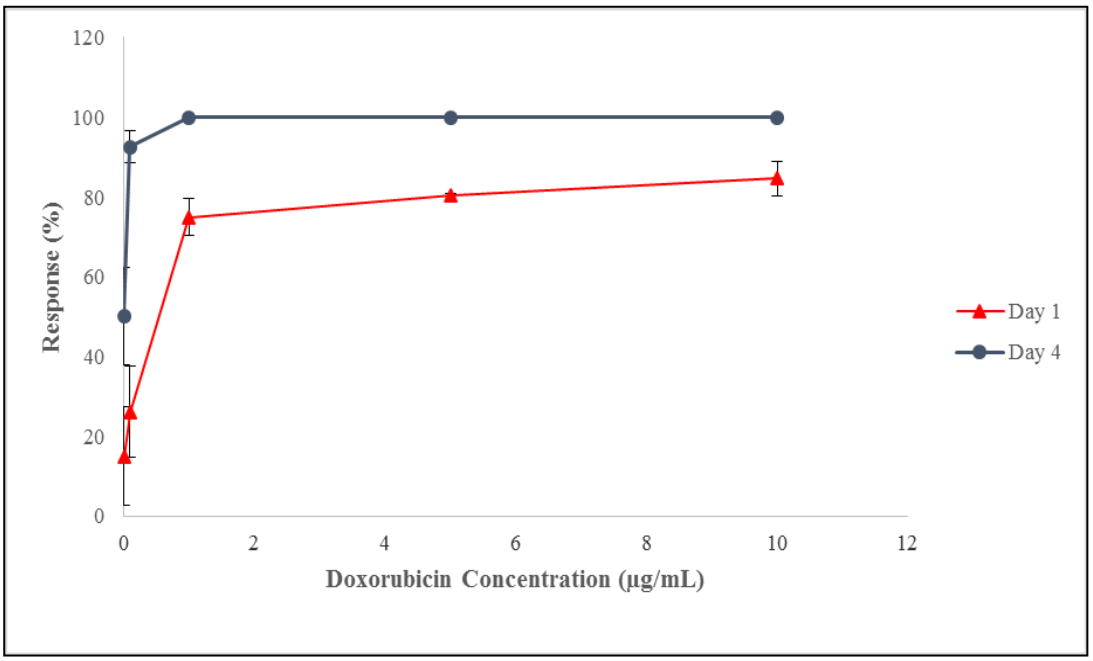

Figure 21. Dose-Response (% cell death) curves for the antiproliferative effect of free doxorubicin on Days 1 and 4. Test medium: RPE/D407 cells ($3x10^4$ cells/well).

It was found that IC_{50} was approximately 0.45 µg/mL on day 1 while 0.01 µg/mL was enough for inhibition of 50% of the cells after 4 days and these data are in accordance with the results of Kuo et al. (2007). Day 2 and 3 yielded the same data as Day 4, and were not shown on Figure 21. Besides that, it was observed that the slope of the dose-response curve was very sharp, indicating a narrow therapeutic range of free doxorubicin (Kuo et al., 2012).

3.2.2 Effect of PC:CHOL (7:3) and PC:CHOL:ATR (7:1:3) Liposomes on RPE/D407 Cell Viability

Liposomes are widely used as a drug carrier system due to their biocompatibility and non-toxicity, in addition to other features. On the other hand, recently cytotoxic effect of all-trans retinal on RPE cells was reported (Maeda et al., 2009). Thus, an adverse effect of photosensitive ATR carrying liposomes on RPE/D407 cell proliferation was expected. Figures 22 and 23 present the effect of different concentrations (0.01, 0.1, 1.0, 5.0, 10.0 µg/mL) of PC:CHOL (7:3) and PC:CHOL:ATR (7:1:3) liposomes without any doxorubicin on RPE/407 cell proliferation, respectively.

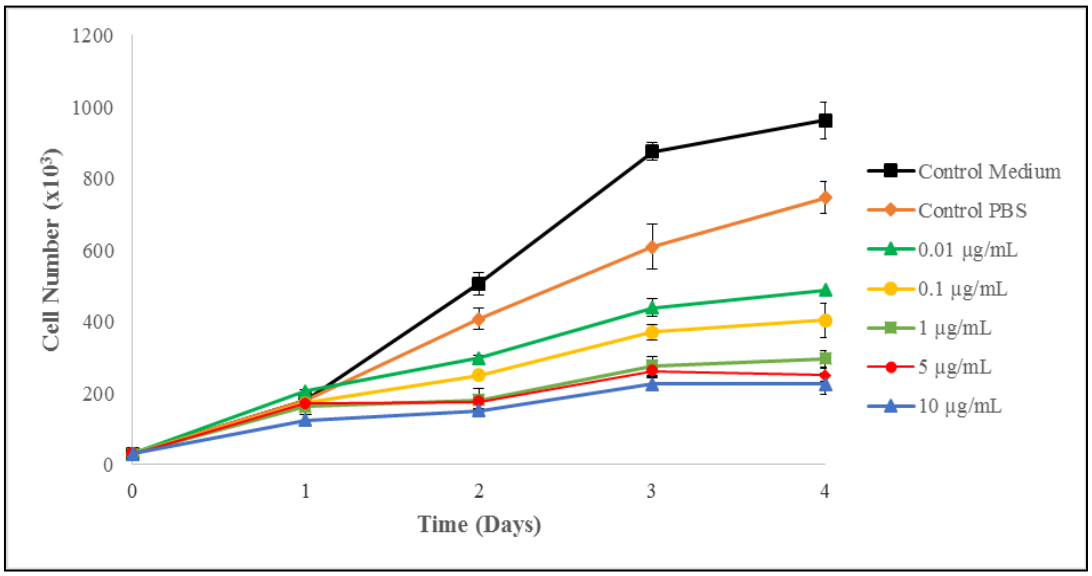

Figure 22. Effect of PC:CHOL (7:3) liposome concentration on RPE/D407 cell viability without doxorubicin loading. Control Medium: RPE/D407 cells incubated in the cell culture medium without any liposome; Control PBS: RPE/D407 cells incubated in the PBS added cell culture medium at the highest volume of liposome.

Figure 22 shows that PC:CHOL (7:3) liposomes have an adverse effect on RPE/D407 cell proliferation as reflected as a decrease in the rate of cell proliferations with increasing liposome concentrations. This might be due to restriction of oxygen diffusion and nutrient transfer in the medium caused by liposomes floating in large amounts in the medium.

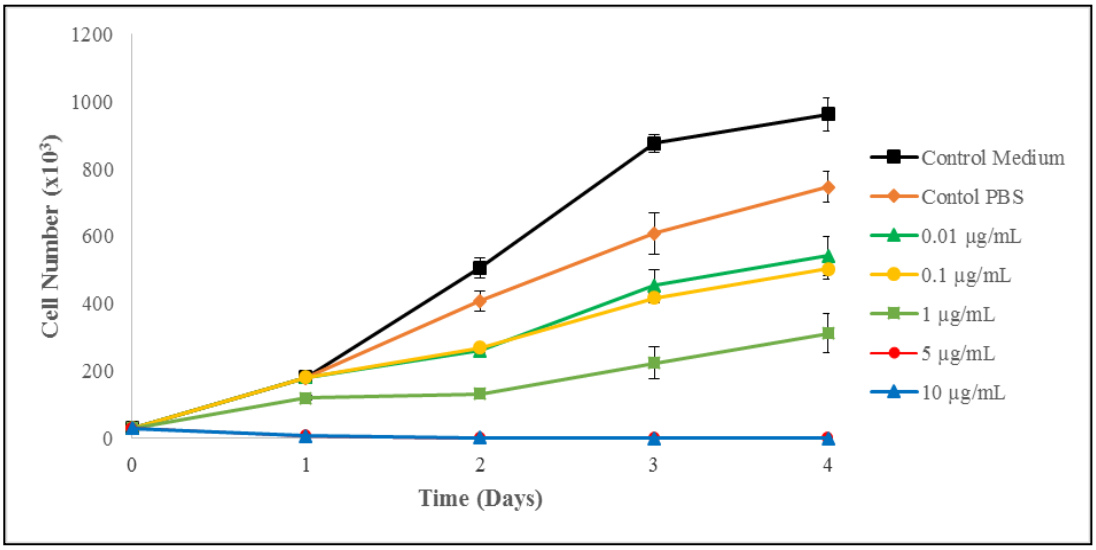

Figure 23. Effect of PC:CHOL:ATR (7:1:3) liposome concentration on RPE/D407 cell viability without doxorubicin loading. Control Medium: RPE/D407 cells incubated in the cell culture medium without any liposome; Control PBS: RPE/D407 cells incubated in the PBS added cell culture medium at the highest volume of liposome**.**

The data presented in Figure 23 is very similar to Figure 22 except that the liposomes contain ATR (PC:CHOL:ATR, 7:1:3), the negative effect of all-trans retinal (ATR) carrying liposomes were observed for higher than 1 µg/mL liposome concentrations, but the first three concentrations (0.01, 0.1 and 1 µg/mL) were in effective in comparison to PC:CHOL (7:3) liposomes. However, for the 5 and 10 µg/mL there is a distinct decrease due to ATR presence (Figure 23). In the literature, adverse effect of all-trans retinal on RPE cell proliferation was explained with reduction of the metabolic activity of the cells in the presence of all-trans retinal (Wielgus et al., 2011). Berchuck et al. (2013) showed that RPE cells express membrane complement regulatory proteins (mCRPs) including CD46 and CD59 on their surface. Deficiency in these mCRPs causes an increase in the sensitivity of cells to cell stress and death. They reported that all-trans retinal caused down regulation of the CD46 and CD59 and decreased their expression by about 50%, so that RPE cells must have become more susceptible to cell death. Therefore, the results about the effect of PC:CHOL:ATR (7:1:3) liposomes on RPE/D407 cell viability are in agreement with the literature.

3.2.3 Effect of Doxorubicin Carrying PC:CHOL:ATR (7:1:3) Liposomes on RPE/D407 Cell Viability

Doxorubicin loaded PC:CHOL:ATR (7:1:3) liposomes were introduced into the cell culture at different concentrations (0.01, 0.1, 1.0, 5.0, 10.0 μg/mL) to observe the effect of doxorubicin released from PC:CHOL:ATR (7:1:3) liposomes on RPE/D407 cells. Half of the liposome suspension was kept in dark at room temperature, while the other half of the liposome suspension was exposed to UVA for 45 min (365 nm, 99 μWatts at a distance of 16 cm) before being added into the cell culture medium. Figures 24 and 25 present the effect of different concentrations (0.01, 0.1, 1.0, 5.0, 10.0 μg/mL) of doxorubicin loaded UVA unexposed and UVA exposed PC:CHOL:ATR (7:1:3) liposomes on RPE/407 cell proliferation, respectively.

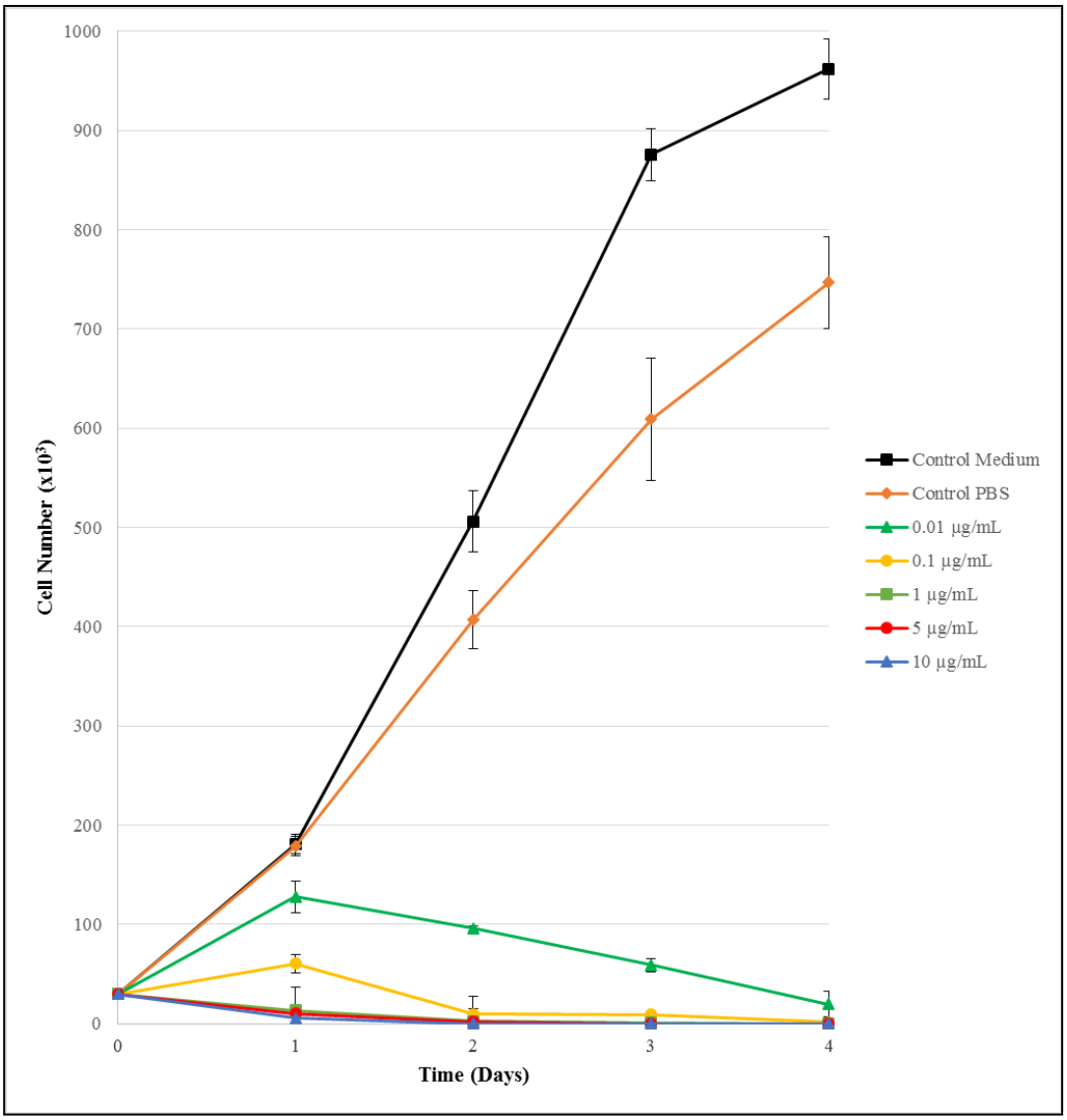

Figure 24. Effect of UVA unexposed PC:CHOL:ATR (7:1:3) liposomal doxorubicin on RPE/D407 cell viability. Control Medium: RPE/D407 cells incubated in the cell culture medium without any liposome; Control PBS: RPE/D407 cells incubated in the PBS added cell culture medium at the highest volume of liposome.

Figure 24 shows that UVA unexposed, 0.01 and 0.1 µg/mL doxorubicin loaded PC:CHOL:ATR (7:1:3) liposomes lead to decrease in the proliferation rate of RPE/D407 cells on Day 1. However, it is seen that 1, 5 and 10 µg/mL doxorubicin loaded PC:CHOL:ATR (7:1:3) liposomes have an antiproliferative effect on the cells.

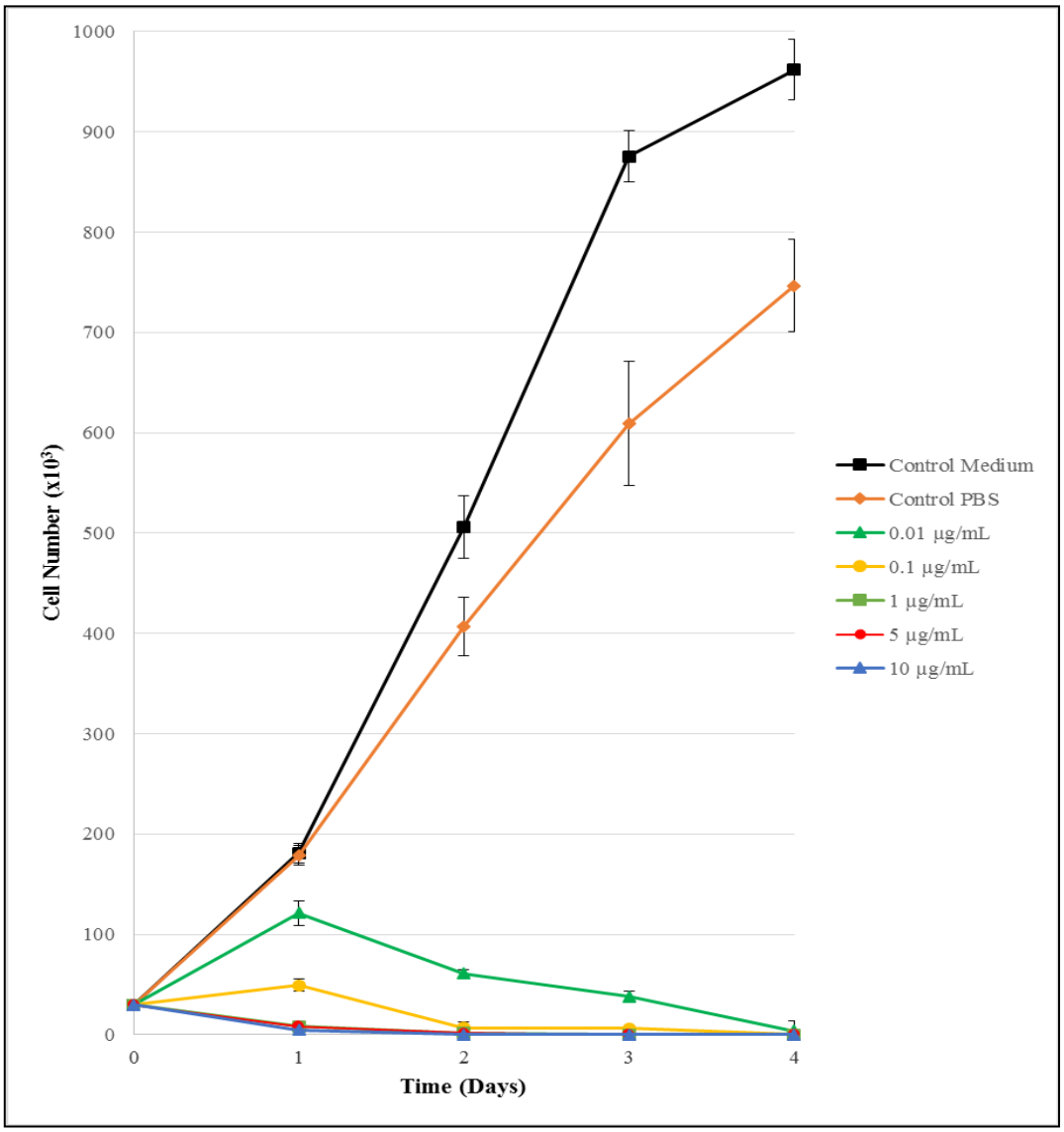

Figure 25. Effect of UVA exposed PC:CHOL:ATR (7:1:3) liposomal doxorubicin on RPE/D407 cell viability. Control Medium: RPE/D407 cells incubated in the cell culture medium without any liposomes; Control PBS: RPE/D407 cells incubated in the PBS added cell culture medium at the highest volume of liposome.

In Figure 25, UVA exposed doxorubicin loaded PC:CHOL:ATR (7:1:3) liposomes have an antiproliferative effect on the cells in a concentration dependent manners as the concentration increased from 0.01 to 10 µg/mL the antiproliferative effect increased. The effect of UVA exposure on the cell response cannot be observed clearly in Figures 24 and 25. Therefore, dose-response graphs were plotted to determine the effect of UVA exposure on RPE/D407 cell viability (Figure 26).

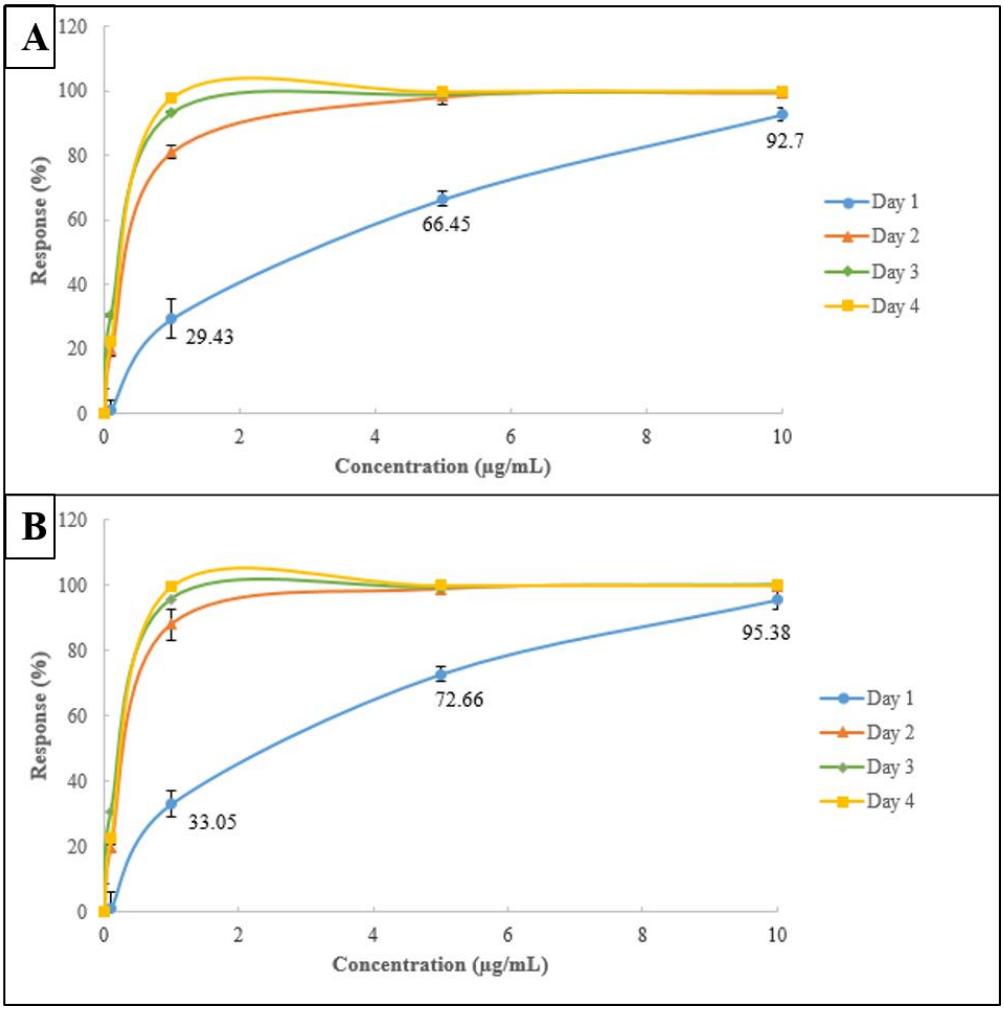

Figure 26. Dose-response curves of RPE/D407 cells for photoresponsive liposomal doxorubicin A) UVA unexposed PC:CHOL:ATR (7:1:3) liposomes, B) UVA exposed PC:CHOL:ATR (7:1:3) liposomes.

In Figure 26, no significant difference could be detected between the UVA unexposed and UVA exposed liposomes for the Days 2, 3 and 4 in terms of cell response. However, for Day 1, the effect of doxorubicin upon UVA exposure showed a slight increase of about 4%. In fact, a more significant difference was expected according to the results of *in situ* release profile of doxorubicin from PC:CHOL:ATR (7:1:3) liposomes (section 3.1.4). This smallness of the difference was thought to be caused by the strong cytotoxic effect of all-trans retinal with respect to doxorubicin.

3.2.4 Cellular Uptake

3.2.4.1 Flow Cytometry Analysis

Flow cytometry analyses were performed in order to study the cellular uptake of empty PC:CHOL:ATR (7:1:3) liposomes, and also the free doxorubicin and doxorubicin loaded PC:CHOL:ATR (7:1:3) liposomes. RPE/D407 cells ($3x10^5$) were incubated with these liposomes with the same concentration 1 μg/mL, for 4 h in an CO_2 incubator (section 2.2.3.2.1). DRAQ5 was used for nuclei staining to get distinct signals from cells. DRAQ5 and doxorubicin were excited with 640 nm and 488 nm lasers and detected with FL4A and FL2A detectors, respectively. All-trans retinal in PC:CHOL:ATR (7:1:3) liposomes was excited with 488 nm laser and detected with FL2A detector. Figure 27 presents the dot plots of FL4A versus FL2A.

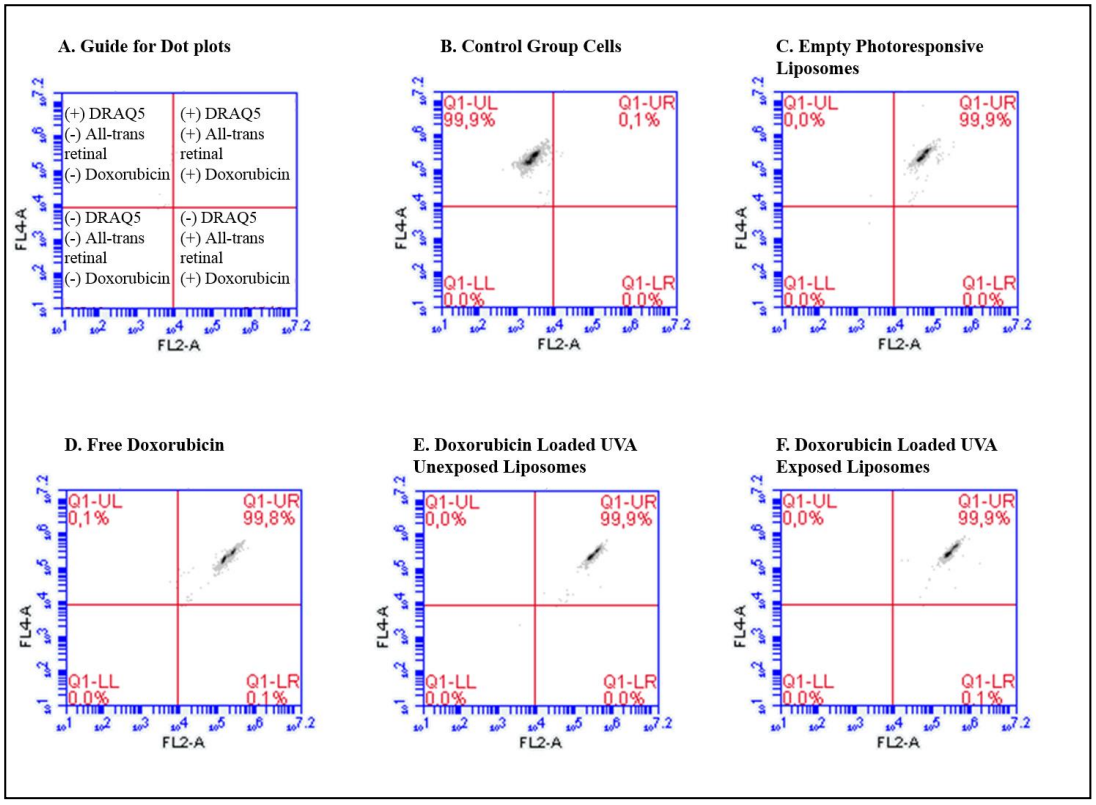

Figure 27. Dot plots for the cellular uptake studies. A) Guide for dot plots, B) Control group cells, C) Empty PC:CHOL:ATR (7:1:3) liposomes, D) Free doxorubicin, E) UVA unexposed doxorubicin loaded PC:CHOL:ATR (7:1:3) liposomes, and F) UVA exposed doxorubicin loaded PC:CHOL:ATR (7:1:3) liposomes. For FL2A $\lambda_{ex.}$ 488 nm, λ_{em} 585 ± 40 nm, for FL4A $\lambda_{ex.}$ 640 nm, λ_{em} 675 ± 25 nm.

Figure 27A was plotted as a guide for the dot plots. The lower-left quadrant displays events that are negative for both parameters. The upper-left quadrant contains events that are positive for the y-axis parameter (DRAQ5) but negative for the x-axis parameter (all-trans retinal and doxorubicin). The lower-right quadrant contains events that are positive for the x-axis parameter (all-trans retinal and doxorubicin) but negative for y-axis parameter (DRAQ5). The upper-right quadrant contains events that are positive for both parameters. As seen in Figure 27B, there were signals in the upper-left quadrant which was positive indicator of DRAQ5 and this result showed that DRAQ5 in control group cells did not give any significant fluorescence intensity with excitation 488 nm laser. In Figure 27 C, fluorescence

intensity was seen in upper-right quadrant which indicates signals were due to both DRAQ5 and all-trans retinal for the same specimen and this shows clearly the uptake of PC:CHOL:ATR (7:1:3) liposomes from cells. Also, cellular uptake of free doxorubicin was observed in Figure 27D where the fluorescence signal is seen in the upper-right quadrant. Besides that, in Figures 27E and 27F, it can be observed that doxorubicin loaded PC:CHOL:ATR (7:1:3) liposomes were taken into RPE/D407 cells successfully because the fluorescence intensity shifted to the right direction in comparison with Figures 27C and 27D. These results showed that signals were coming from both doxorubicin and all-trans retinal for the same specimen. In addition with dot plots, these results were supported with histogram in Figure 28.

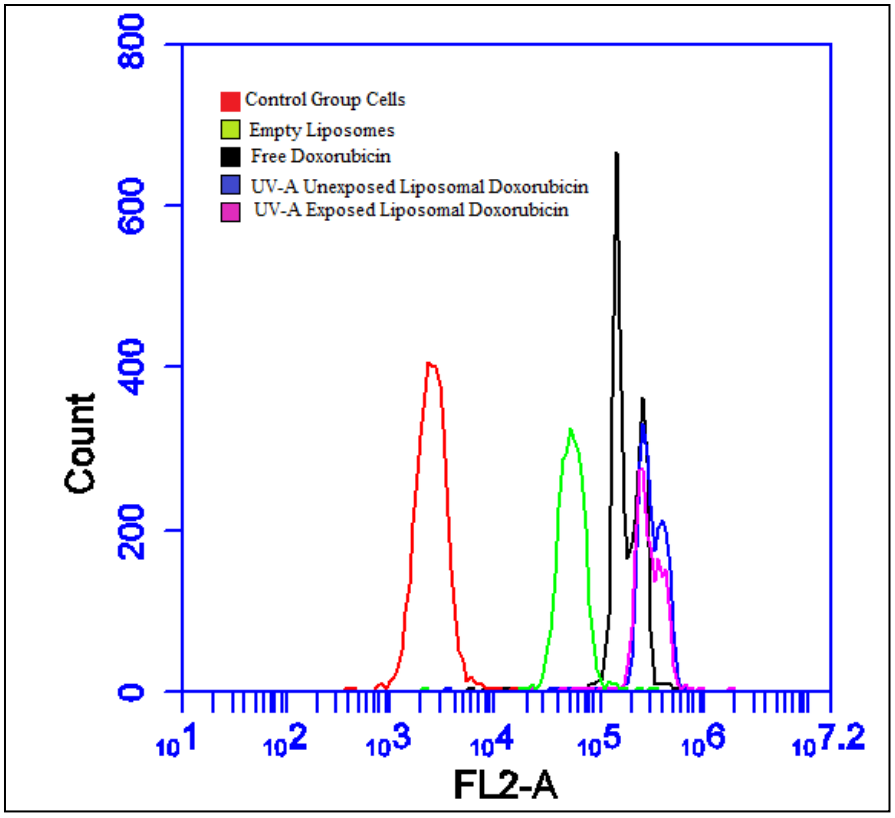

Figure 28. Flow cytometry fluorescence intensity histogram for the uptake into RPE cells. For FL2A $\lambda_{ex.}$ 488 nm, λ_{em} 585 ± 40 nm.

In Figure 28, in the histogram of control group cells, fluorescence intensity is observed between 10^3 and 10^4 with FL2A detector and this value has no significance

for the detection with FL2A as it was shown in Figure 26B before. Therefore, the histogram of control group cells could be taken as a reference. The RPE/D407 cells incubated with empty PC:CHOL:ATR (7:1:3) liposomes show a shift towards higher fluorescence intensity, indicating cellular uptake of empty PC:CHOL:ATR (7:1:3) liposomes. The mean fluorescent intensity of free doxorubicin, and liposomal doxorubicin were also much higher than the mean fluorescence intensity of the control group. It is also observed that the mean fluorescence intensity of liposomal doxorubicin is higher than the mean fluorescence intensity of PC:CHOL:ATR (7:1:3) empty liposomes and free Doxorubicin. Therefore, it is concluded that this high fluorescence intensity results from both all-trans retinal and doxorubicin for the same specimen which supports the cellular uptake of liposomal doxorubicin.

3.2.4.2 Confocal Laser Scanning Microscopy (CLSM)

The interactions of RPE/D407 cells with empty PC:CHOL:ATR (7:1:3) liposomes, free doxorubicin and doxorubicin loaded PC:CHOL:ATR (7:1:3) liposomes were studied with CLSM. RPE/407 cells were seeded onto cover slips in each well of 6 well plates ($3x10^4$ cells/well) and incubated with empty PC:CHOL:ATR (7:1:3) liposomes, free doxorubicin or liposome loaded doxorubicin with the same concentration, 1 μg/mL, for 4 h in a CO_2 incubator as mentioned in section 2.2.3.2.2. Argon lasers at 635 nm and 488 nm were used to excite DRAQ5 (stain for nuclei) and doxorubicin, respectively. All-trans retinal was also excited at 488 nm. The emission band width for DRAQ5 was 645-800 nm, whereas it was 498-560 nm for doxorubicin and all-trans retinal. Figure 29 presents CLSM micrographs of control group cells stained with DRAQ5.

CLSM micrographs in Figure 29A indicate that there is a fluorescence signal due to DRAQ5 excited with 635 nm laser, but, the specimen has not given any fluorescence signal excitation with 488 nm laser (Figure 29B). Cell boundaries and nuclei can be observed in the transmission micrograph (Figure 29C). In Figure 29D, it is observed that RPE/D407 cells do not give any fluorescence signal with excitation 488 nm laser and 488 nm laser also did not excite DRAQ5.

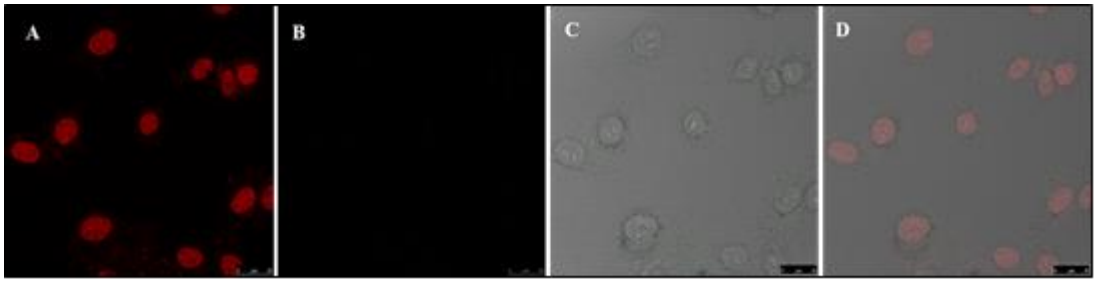

Figure 29. CLSM micrographs of control group RPE/D407 cells staining with DRAQ5. A) Confocal micrograph with 635 nm laser, B) Confocal micrograph with 488 nm laser, C) Transmission micrograph, D) Overlay micrograph. Magnification x40.

Figure 30 shows the CLSM micrographs of interaction between RPE/D407 cells and empty PC:CHOL:ATR (7:1:3) liposomes, free doxorubicin, doxorubicin loaded UVA unexposed and UVA exposed PC:CHOL:ATR (7:1:3) liposomes.

In Figures 30A and 30B, nuclei of RPE/D407 cells were stained with DRAQ5 and fluorescence of doxorubicin in cytoplasmic region can be seen clearly. Figure 30C shows the overlay micrograph which indicates that empty PC:CHOL:ATR (7:1:3) liposomes were taken up by the cells and localized in the cytoplasm but not in the cell nucleus. These results indicate that liposomes protect the drug from the enviroment and carry them effectively into the cell. In Figures 30 D and E, the fluorescence of both DRAQ 5 and doxorubicin are seen in the nuclei. It is observed that, both DRAQ5 and doxorubicin signals are entirely overlapped, indicating that free doxorubicin is localized in the cell nucleus instead of accumulating in the cytoplasm; this is probably due to the tropism of doxorubicin to the cell nucleus (Wang et al., 2012). In Figures 30 G-I, there is fluorescence signal coming from both doxorubicin and all-trans retinal. It is thought that fluorescence signal in the cytoplasmic region is due to all-trans retinal in PC:CHOL:ATR (7:1:3) liposomes, while the signal in the nucleus is due to released doxorubicin. It can be deduced from these micrographs that doxorubicin released from the liposomes reacted with cell nuclei while the liposomes localized in the cytoplasm. In Figures 30 J-L a green fluorescence is seen in both the cytoplasmic and nuclei regions which indicates the localization of released doxorubicin in the nuclei. As a result of CLSM, it is thought that liposomes reacted with RPE/D407 cells and drug molecules were carried safely

into the cells by the liposomes. It is, however, not known if the liposomes are taken up into the cells intact or not.

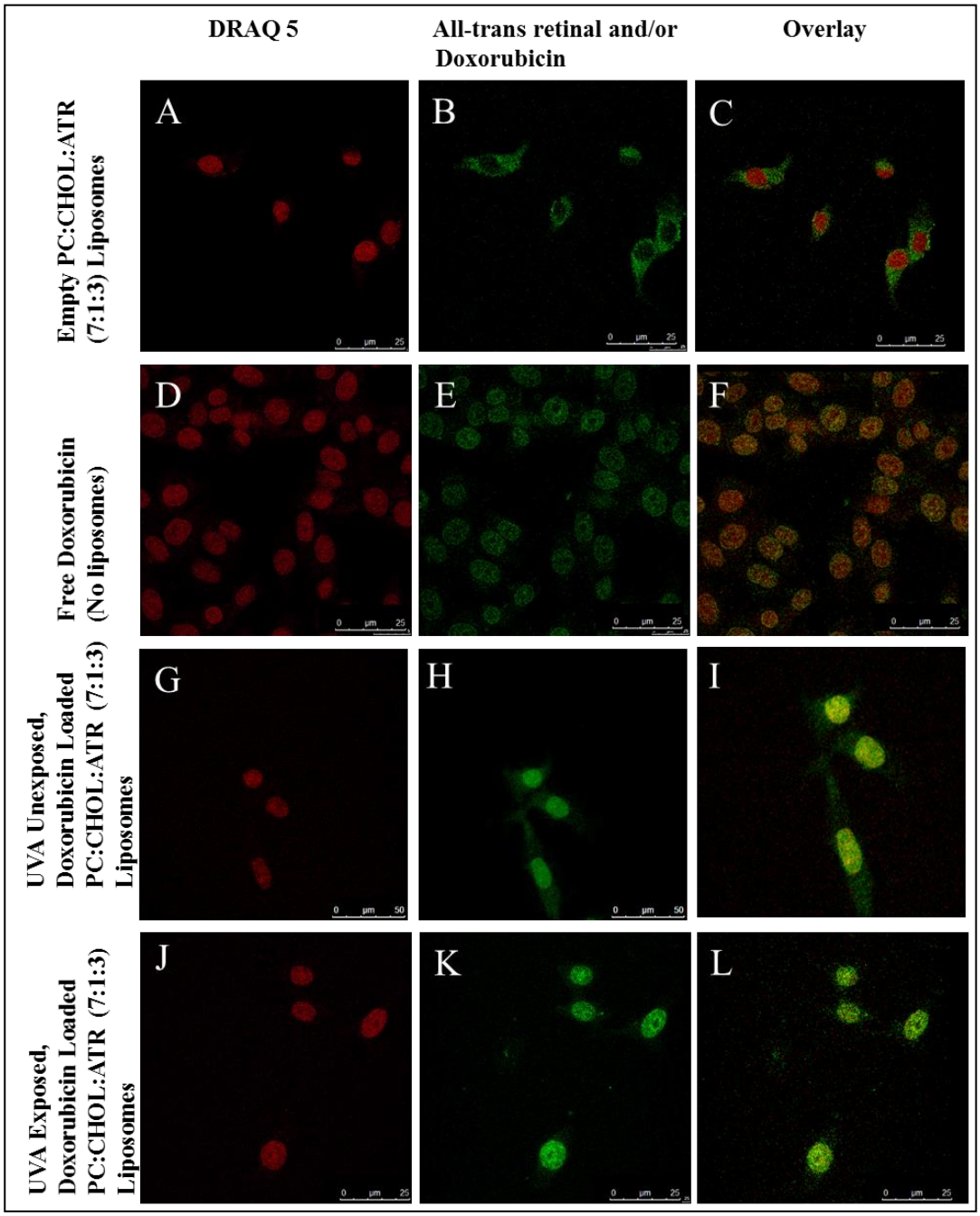

Figure 30. CLSM micrographs of RPE/D407 cells incubated with empty (free of doxorubicin) PC:CHOL:ATR (7:1:3) liposomes (A-C), free doxorubicin (D-F), UVA unexposed doxorubicin loaded PC:CHOL:ATR (7:1:3) liposomes (G-I), and UVA exposed doxorubicin loaded PC:CHOL:ATR (7:1:3) liposomes (J-L). (Red: DRAQ 5, Green: All-trans retinal and doxorubicin). Magnification x40.

CHAPTER 4

CONCLUSION

In this study, three different vitamin A derivatives (9-cis retinal, all-trans retinal and retinoic acid) were incorporated in the phospholipid bilayer of the liposomes to develop photoresponsiveness. Encapsulation efficiency and release studies indicated that each of vitamin A derivatives could be introduced to the liposome structure successfully, but only PC:CHOL:ATR (7:1:3) liposomes showed effective photoresponsiveness possibly due to photoisomerization of ATR to its 13-cis isomer, and so PC:CHOL:ATR (7:1:3) liposome composition was used in the following studies.

The effects of ATR and doxorubicin on RPE/D407 cell viability were studied with Alamar Blue Cell Proliferation Assay and acording to the results, it was seen that ATR had an antiproliferative effect increasing with the concentration of ATR. Free doxorubicin showed an antiprolifrative effect on the cells, too. Doxorubicin released from PC:CHOL:ATR (7:1:3) liposomes decreased the cell numbers in both cases; when exposed to UVA or not. In fact, there were two different bioactive agents in one construct. Apparently the inhibitory effect of ATR was stronger than that of extra doxorubicin released with UVA exposure.

Flow cytometry and confocal microscopy showed that the liposomes or at least the ATR can penetrate the cells and doxorubicin penetrates the nucleus, too, showing why the dual effect was very effective.

REFERENCES

Akbarzadeh A., Rezaei Sadabady R., Davaran S., Joo S. W., Zarghami N., Hanifehpour Y., Nejati Koshki K. (2013). Liposome: classification, preparation, and applications. Nanoscale Research Letters, 8(1), 102–110.

Berchuck J. E., Yang P., Toimil B. A, Ma Z., Baciu P., Jaffe G. J. (2013). All-trans-retinal sensitizes human RPE cells to alternative complement pathway-induced cell death. Investigative Ophthalmology and Visual Science, 54(4), 2669–77.

Borhani H., Peyman G. A., Rahimy M.H. (1995). Suppression of experimental proliferative vitreoretinopathy by sustained intraocular delivery of 5-FU. International Ophthalmology, 19(1), 43–49.

Bozan E., Gurelik G. (2004). Proliferatif Vitreoretinopati Tedavisinde Yeni Deneysel Ajanlar. Ret-Vit, 214–223.

Chang Y.C., Hu D.N., Wu W.C. (2008). Effect of oral 13-cis-retinoic acid treatment on postoperative clinical outcome of eyes with proliferative vitreoretinopathy. American Journal of Ophthalmology, 146(3), 440–446.

Charteris D.G. (1995). Proliferative vitreoretinopathy: pathobiology, surgical management, and adjunctive treatment. The British Journal of Ophthalmology, 79(10), 953–960.

Chen C., Han D., Cai C., Tang X. (2010). An overview of liposome lyophilization and its future potential. Journal of Controlled Release: Official Journal of the Controlled Release Society, 142(3), 299–311.

Cirli O. O., Hasirci V. (2004). UV-induced drug release from photoactive REV sensitized by suprofen. Journal of Controlled Release: Official Journal of the Controlled Release Society, 96(1), 85–96.

Cutts S. M., Nudelman A., Rephaeli A., Phillips D. R. (2005). The power and potential of doxorubicin-DNA adducts. IUBMB Life, 57(2), 73–81.

De Jong W. H., Borm P. J. A. (2008). Drug delivery and nanoparticles: applications and hazards. International Journal of Nanomedicine, 3(2), 133–49.

Dhandapani N. V., Thapa A., Sandip G., Shrestha A., Shrestha, N. (2013). Liposomes as novel drug delivery system: A comprehensive review. International Journal of Research in Pharmaceutical Sciences, 4, 187–193.

Er Y., PhD Thesis, University Of South Australia, (2005). Liposomes in drug delivery: stability, interfacial interaction and drug release.

Ganta S., Devalapally H., Shahiwala A., Amiji M. (2008). A review of stimuli-responsive nanocarriers for drug and gene delivery. Journal of Controlled Release, 126(3), 187–204.

Garweg J. G., Tappeiner C., Halberstadt M. (2013). Pathophysiology of proliferative vitreoretinopathy in retinal detachment. Survey of Ophthalmology, 58(4), 321–9.

Gursel M., Hasirci V. (1995). Influence of membrane components on the stability and drug release properties of reverse phase evaporation vesicles (REVs): light sensitive all-trans retinal, negatively charged phospholipid dicetylphosphate and cholesterol. Journal of Microencapsulation, 12(6), 661-669.

Hincha D. K., Zuther E., Hellwege E. M., Heyer A. G. (2002). Specific effects of fructo- and gluco-oligosaccharides in the preservation of liposomes during drying. Glycobiology, 12(2), 103–10.

Hui YN, Liang HC, Cai YS, Kirchhof B. (1993). Corticosteroids and daunomycin in the prevention of experimental proliferative vitreoretinopathy induced by macrophages. Graefe’s Archive for Clinical and Experimental Ophthalmology, 231(2), 109–114.

Johnston M. J. W., Edwards K., Karlsson G., Cullis P. R. (2008). Influence of drug-to-lipid ratio on drug release properties and liposome integrity in liposomal doxorubicin formulations. Journal of Liposome Research, 18(2), 145–57.

Kagalkar A. A., Nitave S. A. (2013). Approach on novel drug delivery system. World Journal of Pharmacy and Pharmaceutical Sciences, 2(5), 3449–3461.

Karanth H., Murthy R. S. R. (2007). pH-sensitive liposomes-principle and application in cancer therapy. The Journal of Pharmacy and Pharmacology, 59(4), 469–83.

Kawano K., Takayama K., Nagai T., Maitani Y. (2003). Preparation and pharmacokinetics of pirarubicin loaded dehydration-rehydration vesicles. International Journal of Pharmaceutics, 252(1-2), 73–9.

Kubitschke J., Javor S., Rebek J. (2012). Deep cavitand vesicles-multicompartmental hosts. Chemical Communications (Cambridge, England), 48(74), 9251–3.

Kuo H.K., Chen Y.H., Wu P.C., Wu Y.C., Huang F., Kuo C.-W., Shiea J. (2012). Attenuated glial reaction in experimental proliferative vitreoretinopathy treated with liposomal doxorubicin. Investigative Ophthalmology and Visual Science, 53(6), 3167–74.

Kuo H.K., Wu P.C., Yang P.M., Chen Y.H., Wu Y.C., Hu D.N. (2007). Effects of topoisomerase II inhibitors on retinal pigment epithelium and experimental proliferative vitreoretinopathy. Journal of Ocular Pharmacology and Therapeutics, 23(1), 14–20.

Leung S. J., Romanowski M. (2012). Light-activated content release from liposomes. Theranostics, 2(10), 1020–36.

Maeda A., Maeda T., Golczak M., Chou S., Desai A., Hoppel C. L., Palczewski K. (2009). Involvement of all-trans-retinal in acute light-induced retinopathy of mice. The Journal of Biological Chemistry, 284(22), 15173–83.

Manca M. L.., Sinico C., Maccoioni A. M., Diez O., Fadda A. M., Manconi M. (2012). Composition influence on pulmonary delivery of rifampicin liposomes. Pharmaceutics, 4(4), 590-606.

Morescalchi F., Duse S., Gambicorti E., Romano M. R., Costagliola C., Semeraro F. (2013). Proliferative vitreoretinopathy after eye injuries: an overexpression of growth factors and cytokines leading to a retinal keloid. Mediators of Inflammation, 269787.

Mugabe C., Azghani A. O., Omri A. (2006). Preparation and characterization of dehydration-rehydration vesicles loaded with aminoglycoside and macrolide antibiotics. International Journal of Pharmaceutics, 307(2), 244–50.

Mura S., Nicolas J. (2013). Stimuli-responsive nanocarriers for drug delivery. Nature Materials, 12, 991–1003.

Nounou M. M., El-Khordagui L. K., Khalafallah N. A, Khalil S. A. (2006). In vitro release of hydrophilic and hydrophobic drugs from liposomal dispersions and gels. Acta Pharmaceutica, 56(3), 311–24.

Pastor J. C. (1998). Proliferative Vitreoretinopathy : An Overview. Survey of Ophthalmology, 43(1).

Pennock S., Haddock L. J., Eliott D., Mukai S., Kazlauskas A. (2014). Is neutralizing vitreal growth factors a viable strategy to prevent proliferative vitreoretinopathy? Progress in Retinal and Eye Research, 40, 16–34.

Pommier Y., Leo E., Zhang H., Marchand C. (2010). DNA topoisomerases and their poisoning by anticancer and antibacterial drugs. Chemistry and Biology, 17(5), 421–33.

Raffy S., Teissié J. (1999). Control of lipid membrane stability by cholesterol content. Biophysical Journal, 76(4), 2072–80.

Sadaka A., Giuliari G. P. (2012). Proliferative vitreoretinopathy: current and emerging treatments. Clinical Ophthalmology (Auckland, N.Z.), 6, 1325–33.

Smolyanskaya A., Born R. T. (2012). Materials chemistry: Liposomes derived from molecular vases. Nature, 489, 372–374.

Srikanth K., Gupta V. R. M., Manvi S. R., Devanna N. (2012). Particulate carrier systems. International Research Journal of Pharmacy, 3(11), 22–26.

Ta T., Convertine A. J., Reyes C., Stayton P. S., Tyrone M. (2011). Thermosensitive Liposomes Modified with Poly(N-isopropylacrylamide-co-propylacrylic acid) Copolymers for Triggered Release of Doxorubicin. Biomacromolecules, 11(8), 1915–1920.

Thompson D. H., Gerasimov O. V, Wheeler J. J., Rui Y., Anderson V. C. (1996). Triggerable plasmalogen liposomes: improvement of system efficiency. Biochimica et Biophysica Acta, 1279, 25–34.

Tosi G. M., Marigliani D., Romeo N., Toti P. (2014). Disease pathways in proliferative vitreoretinopathy: An ongoing challenge. Journal of Cellular Physiology, 229, 1577–1583.

Tseng P.L., Liang H.J., Chung T.W., Huang Y.Y. (2007). Liposomes incorporated with colesterol for drug release triggered by magnetic field. Journal of Medical and Biological Engineering, 27(1), 29–34.

Umazume K., Liu L., Scott P. A, Castro J. P. F., McDonald K., Kaplan H. J., Tamiya S. (2013). Inhibition of PVR with a tyrosine kinase inhibitor, dasatinib, in the swine. Investigative Ophthalmology and Visual Science, 54(2), 1150–9.

Wang J., Liu Y., Li Y., Dai W., Guo Z., Wang Z., Zhang Q. (2012). EphA2 targeted doxorubicin stealth liposomes as a therapy system for choroidal neovascularization in rats. Investigative Ophthalmology and Visual Science, 53(11), 7348–57.

Wielgus A., Chignell C., Ceger P., Roberts J. (2011). Comparision of A2E Cyto- and Phototoxicity with all-trans-Retinal in Human Retinal Pigment Epithelial Cells. Photochemical and Photobiological Sciences, 86(4), 781–791.

Yang F., Teves S. S., Kemp C. J., Henikoff S. (2014). Doxorubicin, DNA torsion, and chromatin dynamics. Biochimica et Biophysica Acta, 1845(1), 84–9.

Zadi B., Gregoriadis. G. (2000). A novel method for high-yield entrapment of solutes into small lıposomes. Journal of Liposome Research, 10(1), 73–80.

Zhang H., Wang Z., Gong W., Li, Z., Mei X.(2011). Development and characteristics of temperature-sensitive liposomes for vinorelbine bitartrate. International Journal of Pharmaceutics, 414(1-2), 56–62.

http://webvision.med.utah.edu/book/part-i-foundations/simple-anatomy-of-the-retina/ [last accessed on 03.08.2014]

APPENDIX A

CALCEIN CALIBRATION CURVE

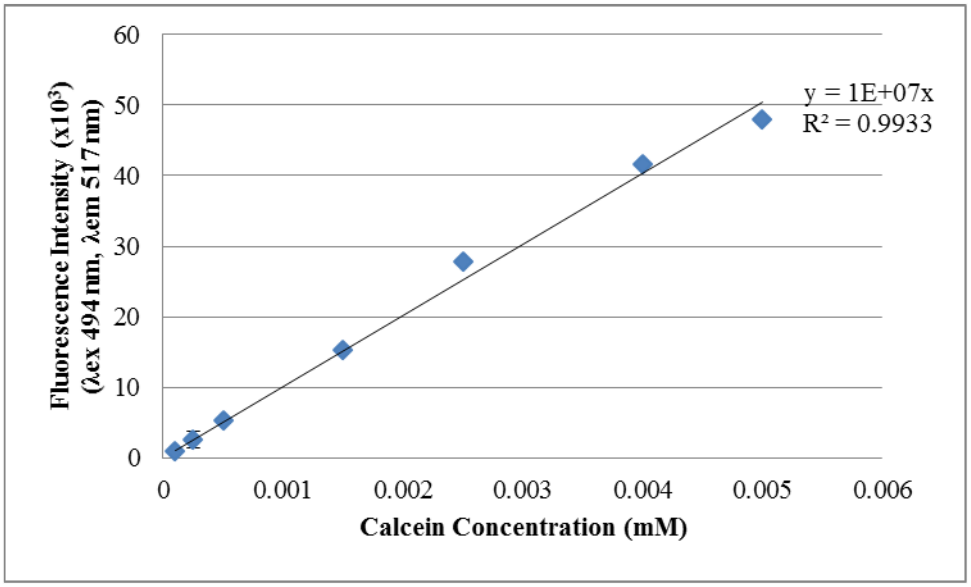

Figure A. Calcein Calibration Curve (n=3)

APPENDIX B

DOXORUBICIN CALIBRATION CURVE

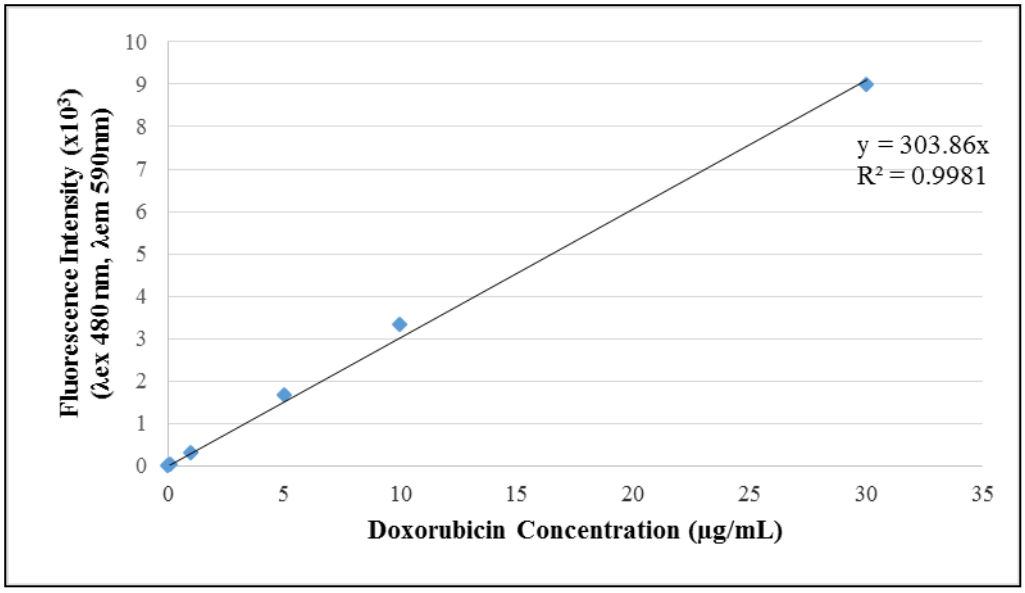

Figure B. Doxorubicin Calibration Curve (n=3)

APPENDIX C

RPE ALAMAR BLUE CALIBRATION CURVE

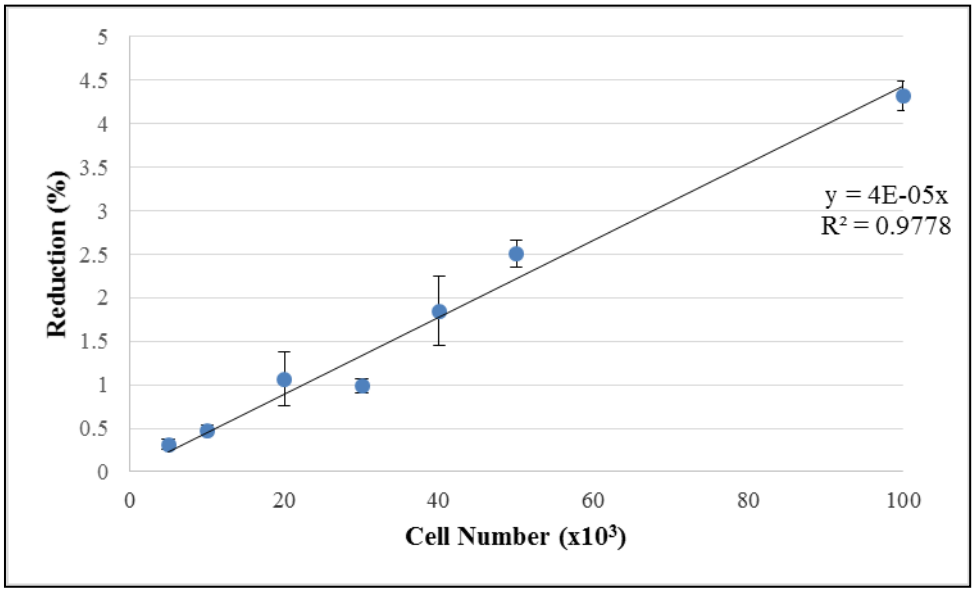

Figure C. RPE Alamar Blue Calibration Curve (n=3)